THESIS

This is to certify that the

thesis entitled

Stability of Response of Canine Tendons to Repeated Elongations.

presented by

Michael Steven Sacks

has been accepted towards fulfillment
of the requirements for

Masters degree in Mechanics

Robert P. Hubbard
Major professor
Robert P. Hubbard

Date 7/31/83

O-7639

MSU is an Affirmative Action/Equal Opportunity Institution

STABILITY OF RESPONSE OF CANINE TENDONS TO REPEATED ELONGATIONS

By

Michael Steven Sacks

A THESIS

Submitted to
Michigan State University
in partial fulfillment of the requirements
for the degree of

MASTER OF SCIENCE

Department of Metallurgy, Mechanics, and Material Science

1983

ABSTRACT

STABILITY OF RESPONSE OF CANINE TENDONS
TO REPEATED ELONGATIONS

By

Michael Steven Sacks

The mechanical response of collagenous tissues to long term repeated elongation is not well understood, and hence requires further investigation. In this study, canine tendons were continuously cycled at a constant strain rate to various strain levels for 2½ hours. Characterization of the mechanical response included behavior of: the peak load, the maximum loading and unloading tangent moduli, the hysteresis, a power fit of the stress-strain curve, and the stability of the above parameters over the length of the test. The peak load and the maximum tangent moduli attained equilibrium values later in the test at higher strain levels. The tendon slack length increased proportionally the same at all strain levels. Power fit coefficients indicated continuous change at all strain levels throughout the test, with greater changes at the lower strain levels. In general, the results indicated that the preconditioning assumption does not hold for long term repeated elongation.

ACKNOWLEDGEMENTS

There were many special people involved in helping in the production and writing of my Master Thesis. I would like here to extend my deep gratitude to them, they are:

Dorothy Rometche, Janet Frahm, Todd Segula, Glenn Beavis, Diane Pietryga, and Richard Geist; undergraduates who relieved me of much burdensome work and made the tissue mechanics lab a very enjoyable place to work.

Robert E. Schaeffer, who's seemingly endless patience and skill kept the sometimes cranky test machinery smoothly working.

Jane Walsh, for doing the fine histological work, and for her warm friendship.

Therese Thelen and Laura Hayes, for doing such a fine job on the seemingly endless chore of typing the manuscript.

The American Osteopathic Association for their generous funding of this project.

Dr. Robert Wm. Soutas-Little, for serving on my committee, for the many favors over my four years in the Biomechanics Department, and for helping to make it a fascinating and enjoyable place to work.

Drs. David Sikarskie and Gary Cloud, for serving on my committee.

My family, for their support in my academic pursuits.

Lastly, but most important; Dr. Robert P. Hubbard, for four years of friendship, guidance, and for establishing a very unique learning experience.

TABLE OF CONTENTS

LIST OF FIGURES

Figure Page

Figure Page

Figure | Page

LIST OF TABLES

Table		Page

I. INTRODUCTION

Knowledge of the mechanical response of connective tissue is necessary to many areas of medical science. Workers in sports medicine, orthopedics, prosthetic development, and related fields all require a thorough understanding of how connective tissues respond under physiological and injurious conditions. Beginning in the 1960's, the mechanical behavior of soft connective tissues, such as tendons and ligaments, have been studied using the experimental and analytical techniques of materials science and continuum mechanics. Works by Fung [1], Viidik [2,3], Crisp [4], Haut and Little [5], Butler, et al. [6], and Harkness [7] all have reported non-linear, viscoelastic responses for collagenous tissues, manifested in a sensitivity for deformation rate and previous deformation history. A summary of the known mechanical response of collagenous tissues follows.

Connective tissues, such as tendons and ligaments, consist of extracellular constituents including: collagen and elastin fibers, and a matrix or ground substance. A definite relationship has been found between the structure of these constituents and their function [Viidik-3]. Experimental evidence is not conclusive on the mechanical role of the ground substance [Yannas-8, Parington and Wood-9]. However, a recent study by Haut [10] indicates that the ground substance in tendon may contribute significantly to its energy absorbtion. In the literature, it is generally agreed that the major stress-bearing component of connective tissues are the collagen fibers, and that the function of the elastin fibers are to bring the tissue back to its original shape when the load is removed. In tendon, collagen fibers are essentially parallel to the long axis of the tendon, and are wavy or helical when not transmitting load. Collagen makes up approximately 75% of the dry weight of a tendon, while elastin only 5% [Elliot-11].

The stress-strain curve for a tendon is commonly divided into four regions, shown in Figure 1 [Butler-6]. As the tendon is first loaded, the lax collagen fibers are not yet straightened, so the mechanical response is due to the elastin fibers (Region I). The degree of strain for which the individual collagen fibers become straight and begin to bear load varies from fiber to fiber [Diamant, et al.-12, Viidik-13]. Thus, as the tendon is extended further, the tissue becomes successively stiffer (Region II). This region will continue until all fibers are straightened, and then a region of apparent constant stiffness begins (Region III). Further extension beyond this region will cause successive fiber rupture and tendon failure (Region IV).

The mechanical response of tendons is impressive: they have an ultimate tensile strength of about 50-100 MPa, and an elongation to failure of 15%-30% [Viidik-2]. These figures can be compared to an aluminium alloy, for which these parameters are 210 MPa and 12%, respectively.

The composition of ligaments varies from predominently collagenous (e.g. cruciate ligaments of the knee) to predominently elastic ligament (e.g. <u>ligamentum</u> <u>flavum</u> of the spinal column). Figure 2 shows typical stress-strain curves for tendon, and collagenous and elastic ligaments. The lower stiffness and greater

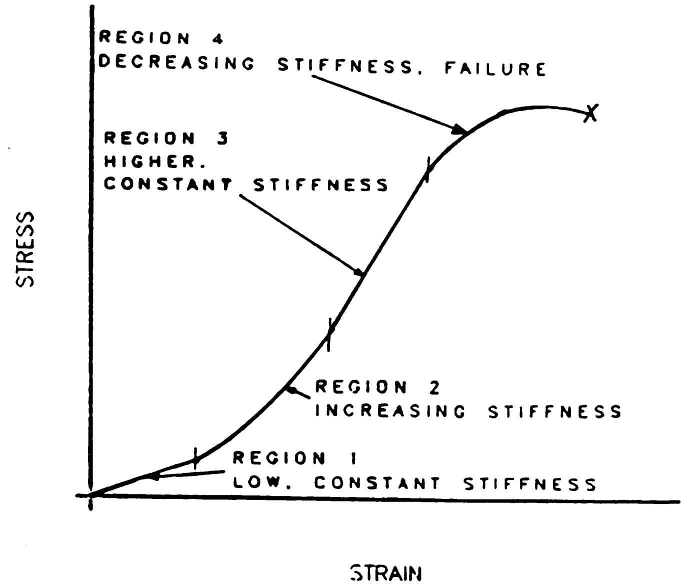

Figure 1 - The four regions of a typical stress-strain curve for tendon.

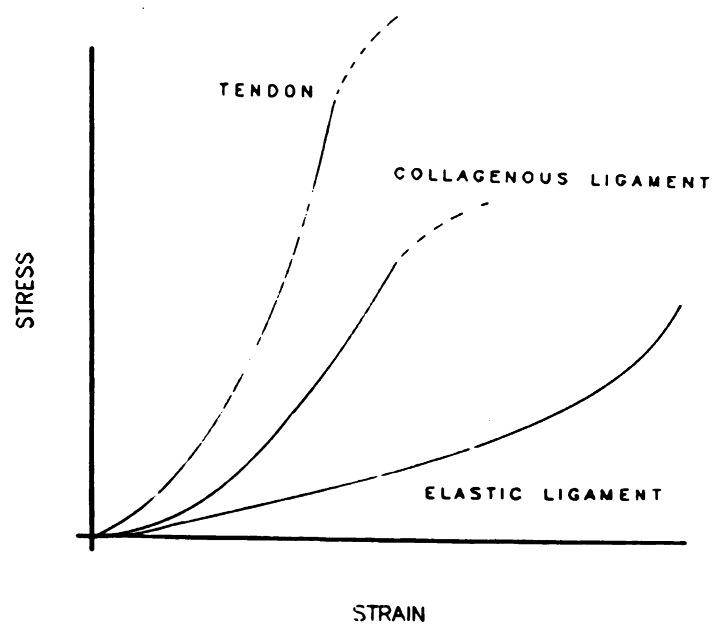

Figure 2 - Typical stress-strain curves for tendon, and collagenous and elastic ligaments.

elongation of tissues which contain more elastin are due to a much lower stiffness of the elastin fibers.

The viscoelastic character of tendons and ligaments is evident in their strain rate, relaxation, and creep behaviors. The general effect of strain rate is an increase in stiffness with an increase in strain rate, as seen for tendon in Figure 3. In relaxation, there is an initial rapid decrease in load, then the decrease in load becomes successively slower as time increases. Several authors [Haut and Little-5, Fung-14, Jenkins and Little-15] have reported an increase in relaxation (initial peak minus an apparent equilibrium load) with an increase in the peak load achieved in the relaxation test. A linear relation has been found between the normalized load (normalized load equals the current load divided by the initial load) and the logarithim of time [Haut and Little-5, Hubbard, et al.-16, Little, et al.-17], in which the slope is a measurement of the degree of relaxation. In creep, tendons and ligaments show a time behavior similar to relaxation, with the strain rapidly increasing initially,

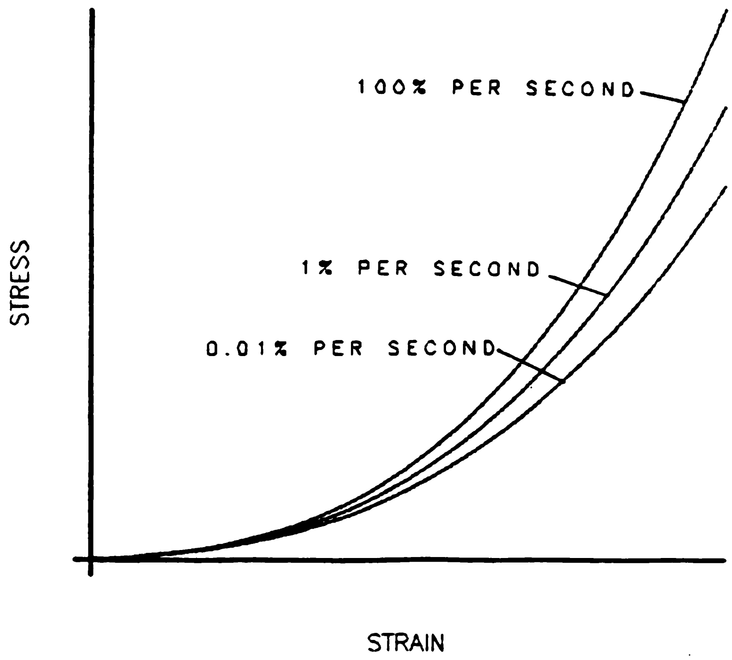

Figure 3 - The effect of varying strain rate on tendon.

than increasing less with time. Cohen [18] has reported an increase in the degree and rate in creep with an increase of load for the human <u>flexor</u> <u>digitorum</u> tendon.

The mechanical properties of tendons and ligaments, like all collageneous tissue, are dependent on their previous mechanical history. This dependence becomes apparent in recovery and preconditioning stability. Recovery is a tendency for the tissues, after a deformation history, to revert to their previous response after a waiting period. The precise cause and character of recovery is not known, however Woo, et al. [19] stated that one hour was appropriate for recovery of the canine <u>medial</u> <u>collaterial</u> ligament at low strains and strain rates (less than 2.5% and 1%/s, respectively). Preconditioning is a property of collagenous tissues that, after a small number of repeated extensions, the tissue's response is stable (i.e. repeatable) from cycle to cycle. This concept is consistent with the thought that when people perform some activity pattern, after a warm-up period, they experience an apparently stable performance of their connective tissues. The most rapid changes in mechanical response occur during initial preconditioning [Viidik-2]. There is a drop in the peak load and hysteresis, as well as an increase in the maximum stiffness. It has been conjectured [Viidik-2, Hubbard, et al.-16] that these changes could be attributed to the upgrading of the parallel alignment of the fibers, as well as a partial redistribution of the ground substance, including water. However, experimental verification for these explanations are lacking.

The stability of the mechanical response following preconditioning is not completely supported by the literature. Fung [1] has stated the need to keep the preconditioning data (e.g. the initial 20 cycles) because of the insufficent understanding of the phenomenon. In a primate spinal ligament study conducted by Little, et al. [20], a test protocol was used that included preconditioning for 10 cycles at 1%/s, with preconditioning stability check cycles throughout the test. Their protocol also included single and cyclic extensions and relaxation tests. A consistent decrease in the peak stress and tangent modulus occured throughout the test sequence (the peak stress decayed often down to 50% of the peak value in the preconditioning cycles). The <u>ligamentum flavum</u>, tested along with other more highly collagenous ligaments, showed smaller decreases in the tangent modulus and peak stress, probably due to the predominance of elastin in the tissue.

Hubbard, et al. [16], in their study of tendons from humans of various ages, showed similar results. Their test protocol was very similar to the spinal ligament protocol, with strains not exceeding 7%. Results showed statistically significant ($p=0.05$) decreases in the peak stress, with the final value (at 9600s) of approximately 65% of the peak stress at the end of preconditioning. The maximum tangent modulus also decreased to a final value of about 85% of its value at the end of preconditioning. Clearly, stable responses do not appear to be reached in the testing protocol used in the above two studies [16, 20].

Several authors have mathematically modeled the mechanical properties of tendons and ligaments, led by Fung [1] who proposed the use of quasi-linear viscoelastic theory to model tissue responses. This approach was based on an earlier modeling of the time dependent elasticity of rubber [Guth, et al.-21]. Haut and Little [5] used Fung's approach to model rat tail tendons, an almost pure source of collagen. The theory was adequate to describe strain rate dependent properties, but in the case of sinusoidal cyclic extensions (run for 15 cycles), it did not agree well with the experimental data. It predicted a much lower peak-load and rate of decay of the peak-loads with time when compared to the experimental data. Similar conclusions were made by Jenkins and Little [15] in the study of the <u>ligamentum nuchae</u>, a predominently elastic ligament. Woo, et al. [19] utilized Fung's theory to model the medial collateral ligament. The test protocol began with preconditioning the sample by cycling it 20 times at a constant strain rate of 0.1%/s, then waiting a one hour recovery period. The sample was then tested at 3 strain rates (.01%/sec, .1%/sec, and 1.0%/sec), with a final check loop at .01%/sec, with one hour periods between each test. Although agreement between theory and experimental data was generally good, in cyclic tests (run for 10 cycles) the theory predicted higher peak and valley stresses than experimental data as time increases. If the cyclic tests had been run longer, the theoretical predictions of Woo, et al., [19] would probably have continued to deviate more from the experimental data.

Recent models for parallel-fibered tissues have taken a micro-structural rather than a phenomenological approach. Lanir [22] assumed that the non-linear response of the tissues is due to the varying lengths of the collagen fibers. He developed a model which utilized a function of the distribution of fiber lengths, and assumed the wavy collagen fibers were linear viscoelastic and are arranged in a planar configuration, with the linear elastic elastin fibers being the sole recrimping agent. A similar model was used by Little, et al. [17] to model spinal ligaments from primates where good agreement was found in the constant strain rate tests. However, they did not attempt to model the relaxation or cyclic creep tests also done in the project.

The above models do not adequately predict the response to cyclic elongation. Yet, the responses of tendons and ligaments to cyclic elongation are central to their biological function. During the course of common activities, people subject their connective tissues to numerous cycles of load and deformation. Playing musical instruments, repetitive work tasks, and sporting activities result in several thousand cycles of mechanical demand on connective tissues. The experimental data for cyclic loading is extremely limited. Most of the existing data is only for short time periods, and only one study by Rigby [23] dealt with long term cyclic extension (greater than 1600s). However, Rigby's results for rat tail tendons indicate an initial drop in the peak stress, then a continued rise to the end of the test (38hrs), conflicting with other studies. The generally poor agreement between available models and existing cyclic data further indicates that the mechanisms involved in cyclic loading are poorly understood. This incomplete understanding of both cyclic response (short and long term) and preconditioning stability, has lead to the present study.

In this study, basic information about the stability of the responses of collagenous tissue to long term cyclic extensions was sought. Three specific questions were addressed:

1) Do connective tissues respond in a consistent or stable manner to repeated extensions?

2) Does stability occur at some levels of cyclic extension and not at others?

3) Are responses after many cycles qualitatively different from the first few cycles?

II. MATERIALS AND METHODS

A. Sample Preparation

Tendon samples were obtained from the hindlimbs of dogs sacrified after veterinary school surgery classes. All hindlimbs were either dissected within a few hours, or refrigerated whole (at 4°C) and dissected within 3 days. The tendons were carefully removed to avoid damage by excessive pulling or by nicking with a scalpel. They were usually cut near the bone insertion point and at the muscle-tendon interface. If the tendon passed over a joint it usually was flared and such a tendon was cut approximately midway in the flared region. The following tendons were used: fibularis longus, flexors digitorum superficialis and profundus, and extensors digitorum longus, lateralis, brevis and communis. These were chosen for their regular geometry, with at least 40 mm of apparently constant cross-sectional area. Thick tendons with diameters greater than 5 mm were avoided, since it was thought that large cross-sections would not insure uniform gripping of the interior fibers during testing.

Upon removal, each tendon was wrapped in a paper towel soaked with Ringers lactate solution (see Appendix A) and sealed in a small plastic bag. Groups of tendons from each dog were put in a larger bag, and these larger bags were put in air-tight containers and stored at -70°C. This method of packing was used to prevent sample dehydration and decay while frozen.

B. Testing Equipment

Tests were performed utilizing an Instron* servohydraulic materials testing machine, which could be computer controlled. The

*Model 1331, Instron Corp, Canton Mass.

actuator was mounted in the upper crosshead and the load cell was mounted within the immersion bath, between the lower grips and the lower crosshead. By having the load cell not mounted between the upper grips and the actuator, noise in the load signal from actuator motion and vibration was greatly reduced. The actuator has a maximum travel rate of 1 m/sec, more than ample for these tests. The load cell used was a fully submersible Interface SSM-100 448 N (100 pound) cell. An immersion bath was used to facilitate a physiological environment, and eliminate any chance of tissue drying, which would drastically affect the mechanical response.

Gripping, often a difficult problem in soft tissue testing, was done by cementing waterproof 100 grit silicon sandpaper to the grip's inner surfaces. The grips were a simple clamp type, with a gripping surface dimension of 15 mm x 20 mm. This provided ample friction without damaging the sample. Histology done on preliminary tests showed the fibers within the grips to be continuous and compressed together, but neither torn nor fractured.

The computer used for test control and data acquisition and analysis was a Digital Equipment Corp. PDP 11/23; coupled to the computer were 2 RL01 hard disk drives, and 2 RX02 floppy disk drives. An Instron Machine Inteface unit enabled command and data communication between the computer and the testing machine. Data was displayed using a Tektronix 4010-1 graphics terminal and a Printronix P-300 high speed line printer. The graphics routine utilized was MULPLT [29], a powerful data-file based program. Data was also monitored and stored on a Nicolet digital oscilloscope, which had a mini-floppy disk for data storage.

C. Test Protocol

Throughout the preparation and testing, the samples were kept either fully moistened or immersed in Ringers lactate solution at room temperature (22°C). Test preparation began by first removing a sample from the freezer, then placing it still wrapped in the towel into a container filled with Ringers lactate solution at room temperature. The sample was allowed to sit in the container for a minimum of 15 minutes for complete thawing and any osmotic processes to stabilize. The paper towel was removed and the sample placed on a plastic dissection tablet. Next, the tendon sheath was removed with great care to insure no fibers were damaged. The sample was marked with Nigrosin dye approximately every 5 mm, so that deformation and any grip slippage that may have occured could be measured photographically. The tendon sheath was removed because it is not rigidly connected to the tendon fibers and hence may not closely follow fiber movement.

Testing began by mounting the prepared sample into the upper grip, then lowering it into the lower grip and securing it. The front cover plate of the immersion bath was mounted and the bath filled. With the sample slack, the load reading was electronically zeroed by adjusting offset controls on the Instron load controller. Carefully monitoring the load signal on the Nicolet, the sample was slowly extended until a load of 0.004 N (typically a stress of 2 KPa) was achieved, the smallest load measureable by the equipment. The length of the sample at this point was taken to be its initial length, and a photograph was taken. The values for the initial length, strain level required for testing, and the computer file names were entered into the testing progam for computer control.

The testing involved cyclic extensions at a constant rate, with the maximum extension held constant. Maximum strains of 2%, 3%, 4%, and 6% were chosen to study strain level sensitivity. Strain rate sensitivity was not investigated in this study, and a constant rate of 5%/s was chosen as an intermediate value between rapid and slow physiological movement. A constant strain rate was chosen to eliminate strain rate effects, and to allow a constant number of data samples per percent strain so all strain levels could be analyzed identically. However, by fixing the strain rate, the frequency and total number of extensions varied between strain levels. For the total test time of 9000s, this method resulted in frequencies and total number of extensions of:

a) 1.250 Hz and 11,250 cycles at 2% strain
b) 0.825 Hz and 7,500 cycles at 3% strain
c) 0.625 Hz and 5,625 cycles at 4% strain
d) 0.417 Hz and 3,750 cycles at 6% strain

Upon test completion, the sample was then extended until a load of 0.004 N was achieved. This was considered to be the final length, and a photograph taken. The sample was then removed and placed into a sealed container filled with Ringers lactate and refrigerated at 4°C.

D. Data Aquisition, Storage, and Analysis

Groups of raw data were taken throughout each test approximately every 70 seconds. Each raw data group consisted of an array of 2,080 data pairs of load and deflection values taken every 6 milliseconds for a total of 12.48 seconds. In order to have continuous load-deflection data for later analysis, the first raw data group and one group every half-hour were written to a raw data file on a hard disk.

A subroutine analyzed each raw data group and generated the following values for each complete cycle within the group:

1. time, deflection, and load value at the load peak
2. loading and unloading energies
3. maximum loading and unloading stiffnesses

These values from each data group were written to a summarized data file on a hard disk. The peak deflection values were not recorded because these values are virtually identical to the deflection at the load peak, except for a short time lag due to the viscoelastic properties of the tendon. The energies were calculated from the areas under the load-extension curves, utilizing a simple rectangular-rule area approximation algorithm. This method was chosen as the most direct, and elimanated the need to presuppose an analytic behavior of the load-extension curves. The maximum stiffnesses were calculated with a linear regression on the last 19 data pairs before the load peak and on the first 19 pairs after the load peak. The 19 data pairs corresponded to the final .57% strain of extension for all tests. A 19 data point "window" was used because it was large enough to filter out the noise in the load-extension curve, yet small enough to obtain an accurate estimate of the maximum stiffness. Both the summary and raw data files were constructed for plotting by MULPLT [24], a data file based computer plotting routine. The load peak-versus-time data were plotted on linear, semilog and log-log axes to see if the load peak-versus-time behavior followed a simple analytic function.

The stress peaks and the maximum tangent moduli (M.T.M.) were converted from the peak load and maximum stiffness, respectively. The peak stress was calculated by dividing the peak load by the cross-sectional area. The maximum tangent moduli were calculated by the following equation:

$$\text{M.T.M.} = (\text{Max. Stf.}) \times \frac{\text{Lo}}{100\text{xA}}$$

where Lo is the initial length, and A is the cross-sectional area. This yields a maximum tangent moduli expressed in MPa per percent strain.

The stability of the stress peaks and the maximum tangent moduli were analyzed by a computer program. This program worked by accessing the summarized data file from a particular test (which contains the above mechanical parameters), and calculating for each data group the mean value, mean time, standard error, and the number of samples for the mechanical parameter considered. It then compared the mean values by checking to see if any two mean values considered were different, doing so in the following manner. Starting at the beginning of the summary file (i.e. the beginning of the test), a particular data group was successively compared to each following data group in order to detect the last data group that was not different from the particular data group. Several different criteria were used to test for a difference between the two means: a t-test at $p=0.05$ [25], which assumed the means had the same population distribution and used a pooled estimate for the standard error, and the difference between the two means being within either 1%, 2%, or 5% of the initial value of the mechanical parameter considered. The latter method was chosen so the time of stabilization could be related to the total change of a mechanical parameter occuring in each test. The objective of the comparison was to find the last data group whose mean value was not different from the mean value of the data group considered, for each of the above criteria. The program created a file of the mean times for each data group within the summary file, and the last data group not different for each data group, for each criterion.

The stabilization program allowed comparisons of the time for stability of a mechanical parameter between both different strain levels and the different criteria within each strain level. For a given criterion in a particular test, the more stable a mechanical parameter was, the sooner in the test the data groups would have the time of the last not different data group equal to 9000s (2.5 hrs, the total time of the test). For ease of analysis, the time of the last data group not different vs. the time of the data group considered were plotted by MULPLT, an example shown in Figure 4. The extremes of the curves can range from a diagonal line to a horizontal line at 9000s. The first extreme curve would indicate a completely unstable parameter, since each data group would be different from all succesive groups. The second would indicate a completely stable parameter, since all data groups would not be different from each other. Indicated on the plot are the times where the data groups were no longer different from the last data group in the test, for each criterion. The times of stabilization were considered to be these times.

Figure 4 - A typical stabilization time plot for the peak stress, loading and unloading Maximum Tangent Moduli, showing the t-test, 2% and 5% difference criteria.

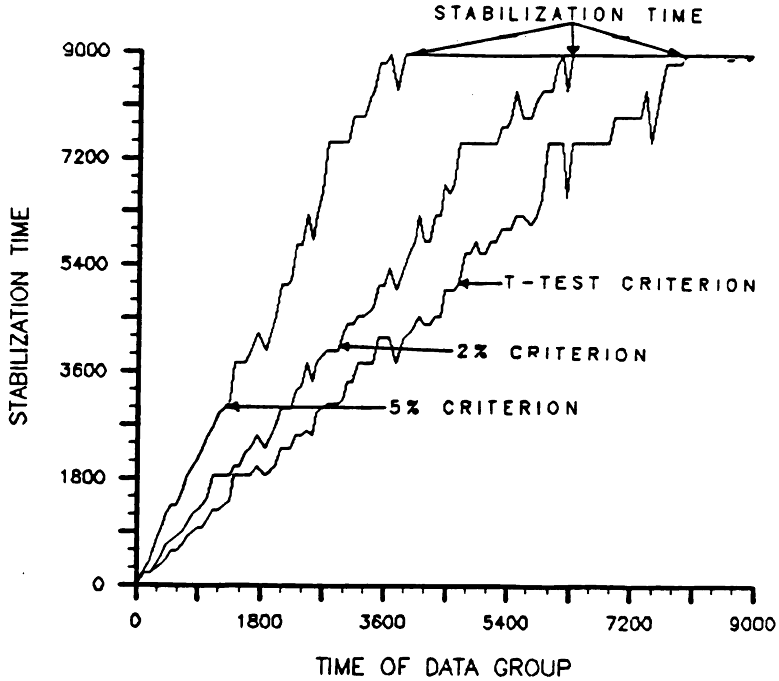

Another program, similar to the stabilization program, was used to perform a linear regression on the peak stress and maximum tangent moduli within each data group. This was done to check if the calculated slopes within each data group were significantly different from zero via a t-test at p=0.05 [25]. If the slope was not different from zero, then the changes in the above mechanical parameters were negliable within each data group, and the mean values calculated for each group were valid.

The stress-strain curves were fitted to a power function of strain. Haut and Little [5] reported, for the rat tail tendon, a high statistical correlation for the power function:

$$\sigma = A\,\varepsilon^{B} \qquad (1)$$

where B had a value of approximately 2, and A a value of approximately 2.0 MPa (σ denotes stress, ε denotes strain). These values were obtained for strains between 0.6% and 1.8%, and for strain rates between .08 and .68%/s.

In the present study, the values for A and B were derived from the experimental data by a least squares regression of the logarithmic expression of equation (1):

$$\log(\sigma + 1) = \log(A) + B \log(\varepsilon - \varepsilon_s + 1) \qquad (2)$$

The offsets of one to the values for stress (σ) and strain (ε) were done to accomodate the initial zero values in the logrithmic fit. ε_s is the smallest strain at which stress deviates from zero (Figure 5), having values starting at zero for the first extension and increasing from cycles to cycle. This regression was done separately on both the loading and unloading curves for: cycles 1-3, 5, the last complete cycle in the first raw data group (at 12s), and on a cycle every half-hour.

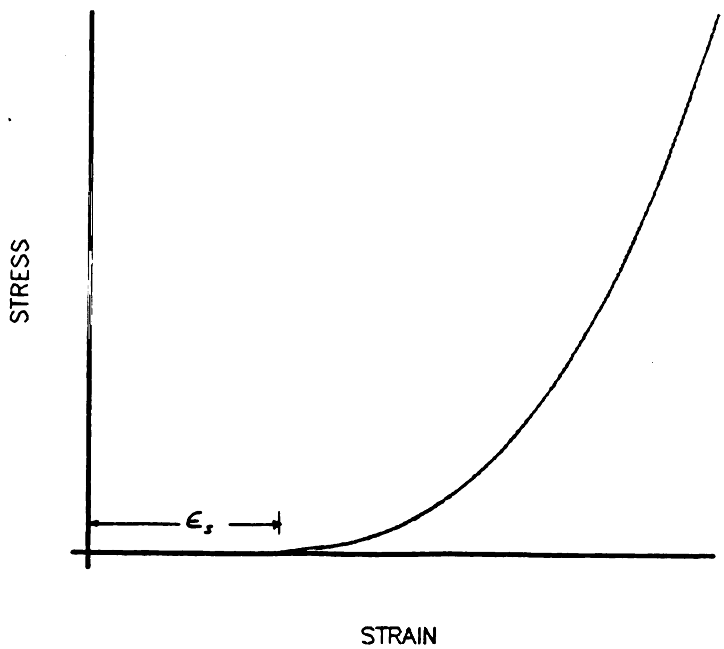

Figure 5 - Definition of the slack strain for a typical stress-strain curve.

In order that statistical changes in the mechanical parameters could be more thoroughly evaluated, a repeated measures technique [26] was used. This involved calculating differences in data for each sample between successive cycles from each test, and then calculating a mean difference for each strain level. Each mean difference was then statistically checked via a Tau-test ($p=0.05$, assuming the means had the same population distribution, see reference 25) to see if it was significantly different from zero. The repeated measures technique was especially useful for data that had a large amount of scatter in the group means, which could mask out any apparent trends among samples.

For the statistical tests for a significant difference between strain levels for the mechanical parameters investigated in this study, a test assuming a Behrens-Fisher distribution [27] was used. This test has a sampling distribution which is neither normal or students (i.e. a t-test distribution). A Cochran and Cox [27] method at $p=0.05$ was used to calculate the critical values for a significant difference between means. This method was utilized because it is ideal for very small samples ($n < 10$), and is generally more sensitive to small differences between means than other available small sample statistical tests.

Load-extension data was also taken and stored for the initial 50 seconds of the test by the Nicolet oscilloscope utilizing its "long sweep" storage mode. This mode allowed 8 continuous sweeps of data to be stored on the mini-floppy. This additional storage by the Nicolet allowed a more complete picture of the initial response then possible by using solely the computer-taken data.

E. Histology, Cross-Sectional Area Calculation, and Slippage Measurements

Within one day of testing, the sample was placed into a mercuric chloride-formalin fix (see Appendix B) for 3 days then removed and pieces desired for histology were cut from the samples. Cross-sections were taken from the center of the sample and from both gripped ends. Longitudinal sections were taken from both ends of the sample to a few millimeters within the gripped area. These sections were then put through a standard slide preparation procedure (see appendix), using Hematoxylin-Eosin stains for the collagen and elastin fibers.

Cross-sectional area was determined by using the slide from the center section of the sample. The slide was first placed into a photographic enlarger to expose the photographic paper along with a glass scale. The area of the photographic image was calculated by an area digitizer and multiplied by the appropriate scale factor measured from the image of the glass scale. Slight size changes that may have occured during the histological processes were thought to be uniform throughout all samples.

The slippage measurements were performed using 8 x 10 prints of photographs of the sample just before and just after testing. The distance from grip to grip, as well as from both grips to the closest dye mark was measured from the print. These measurements were converted to percent changes from the initial to final length. If the sample deformed uniformly throughout the test then all the measurements should increase the same proportional amount. A particularly large change between the closest dye mark and the grip would imply that either slippage or excessive deformation near a grip occured.

III. RESULTS AND DISCUSSION

A. Samples

Table 1 lists the tendon names, and initial lengths and cross-sectional area data for the samples tested. Variations in the initial length and cross-sectional area measurements are fairly uniform throughout the strain levels. A slightly higher initial length occurs at the 2% strain level, due to the selection of larger specimens used here to achieve easily measureable loads at this lowest strain level. Names for several of the tendons were lost due to smearing of the names on the plastic storage bags during freezing and packing, indicated by a (?) in the table. However, these tendons are from the group listed in the materials and methods section. Some problems with testing occured due to static electricity in the Instron's servo-hydraulic system. The actuator would occasionally jump several mm during a test, causing substantial increases in load, data from such tests were discarded. This problem was corrected later on in the testing by improved grounding.

B. Peak Stress

The typical behavior of the peak stress-vs.-time is shown in Figure 6. The extreme strain levels (6% and 2%) are shown, and an exponential-like decay in the peak load with time can be seen in both cases. Although a greater degree of decay (peak minus final load) apppears to occur at the higher strain level (6%), the decay is proportionally about the same at both strain levels. The amount of total cyclic stress relaxation, taken from Table 1, appears to be proportionally equal at all strain levels. Evidently, the amount of

TABLE 1 - Names of Tendons, Initial Lengths, and Cross-Sectional Areas for the Successful Tests*

Strain Level	Tendon		Lo**	Area@	Total Stress Relaxation@@
2%	extensor digitorum lateralis		65.00	2.0838	57
	extensor digitorum brevis		53.00	0.8625	70
	extensor digitorum brevis		50.00	1.1860	68
	flexor (?)		42.00	2.9995	59
	extensor digitorum brevis		30.85	1.1940	55
		Mean	46.64	1.5902	63.17
		S.E.	11.98	0.8025	6.91
3%	extensor digitorum lateralis		28.00	1.8290	53
	(?)		30.00	1.9656	51
	extensor digitorum brevis		44.50	2.5412	63
	(?)		34.00	0.9437	62
	(?)		35.00	1.0172	58
	(?)		19.00	1.3544	40
	extensor digitorum brevis		24.70	0.8169	63
		Mean	30.74	1.4954	55.17
		S.E.	8.17	0.6376	8.44
4%	(?)		39.00	1.0330	63
	fibularus longus		44.50	1.7242	62
	fibularus longus		56.00	1.8802	63
	extensor digitorum brevis		33.90	1.4101	72
	extensor digitorum longus		23.95	1.3097	55
	extensor digitorum longus		22.62	0.6410	70
		Mean	36.66	1.3330	64.17
		S.E.	12.71	0.4534	6.11
6%	tibialis cranialis		37.00	2.7870	60
	flexor (?)		17.05	1.6912	62
	extensor digitorum brevis		21.00	1.0090	60
	extensor digitorum lateralis		27.00	1.6526	50
	extensor digitorum protundus		31.65	1.0630	43
		Mean	26.74	1.6626	55.00
		S.E.	8.00	0.6929	8.19

*—(?) indicates lost indentification

**—$M \times 10^{-3}$

@—$M^2 \times 10^{-6}$

@@—% of initial stress

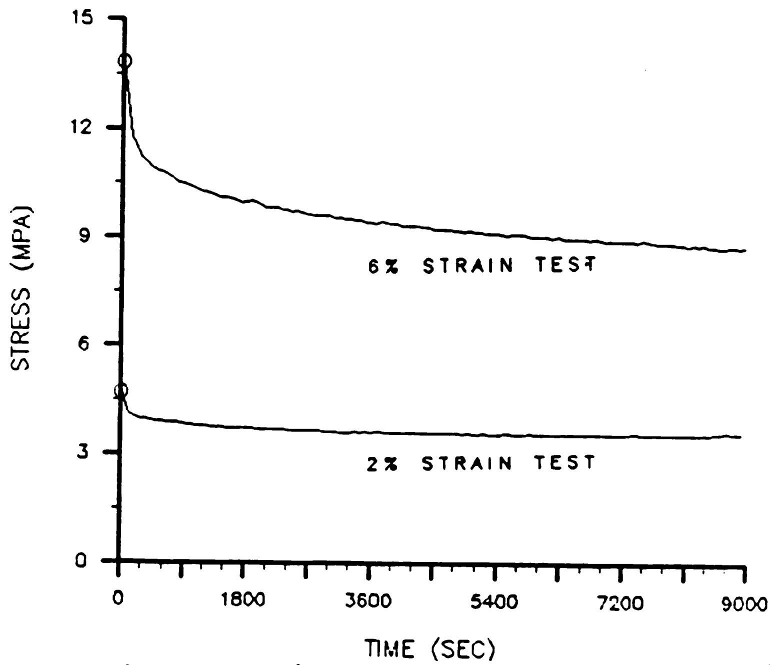

Figure 6 - Typical behavior of the peak stress-vs.-time for a 2% and 6% strain level test.

cyclic relaxation appears to be insensitive to strain level for the range of strain levels tested.

Figure 7 depicts these same 6% and 2% tests plotted on semi-log axis. Clearly, a linear behavior with the log of time does not occur in the 6% test. This non-linearity occured in approximately 60% of the tests, with the curves ranging from almost linear (as seen in the 2% test), to a curve similar to the 6% curve. No consistent behavior was found at any strain level. Plots of log stress-time, and log stress-log time also showed no consistent behavior. Because of this, no curve fitting was performed on the peak-stress vs. time data.

Figure 8 depicts the mean stress peaks for the first and fifth cycles at the strain levels tested, taken from Table 2. The values for 6% strain are comparable to human tendons [Hubbard-16], which attained a peak stress of about 15 MPa at 7% strain; and to primate tendons [Selke, et. al.-28], which attain about 15.3 MPa at 5% strain. In the first cycle data, the values at 2%, 3%, and 4% strain appear to outline an expected non-linear response of the mean stress peaks to strain level. However, the mean at 6% strain, although higher than at 4%, is lower than a smooth non-linear response would produce. This could be due to fiber or fibril damage in the tendon (6% strain could be in Region IV), or to possible slippage.

Peak stress means at the fifth cycle showed marked decreases, with greater decreases occuring at higher strain levels. Statistics on the first and fifth cycle peak stress means, listed in Table 3, indicate significant differences occur at the 6%-2%, 4%-3%, and 4%-2% intervals at both cycles. Because of the large data scatter, the lack of a significant difference at the other intervals may not be very

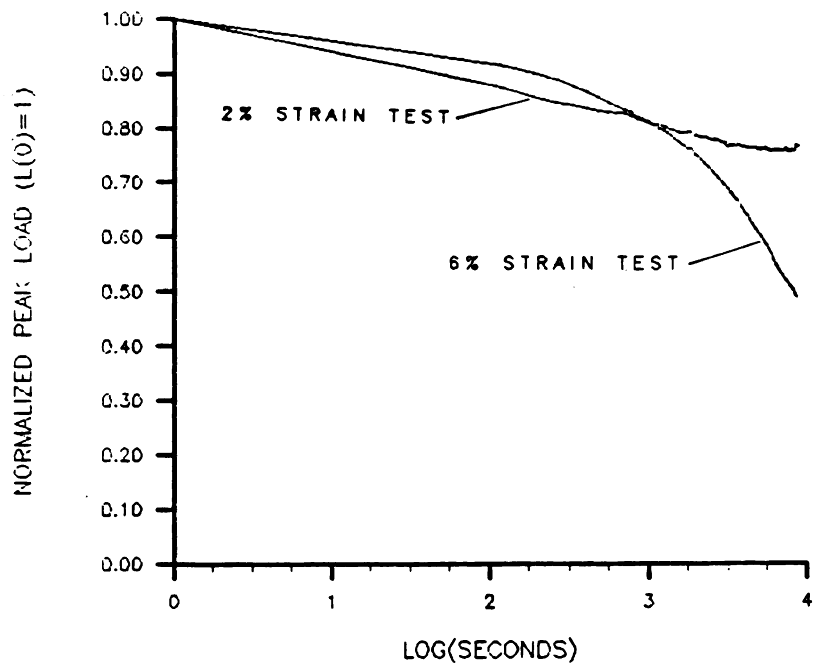

Figure 7 - Typical behavior of the peak stress-vs.-log time for a 2% and 6% strain level test.

TABLE 2 - Results for the Peak Stress, Loading and Unloading Maximum Tangent Moduli (L-M.T.M. and UL-M.T.M., respectively) at the First and Fifth Cycles; and the Loading Offset Strain at the Fifth Cycle

	1st Cycle			5th Cycle			
	Peak Stress (MPa)	L-M.T.M. (MPa/%)	UL-M.T.M. (MPa/%)	Peak Stress (MPa)	L-M.T.M. (MPa/%)	UL-M.T.M. (MPa/%)	Loading Offset Strain at 5th Cycle(%)
2%	3.7034	3.6562	5.4012	3.2929	4.3164	4.8124	1.3542
	2.0451	2.1203	3.2576	1.8377	2.3589	2.9159	1.4298
	5.2391	5.4069	7.6588	4.7534	5.8754	7.3641	1.1951
	7.3448	6.1878	8.6195	6.7411	7.0312	8.2516	1.3086
	0.6271	0.5836	0.9544	0.5474	0.6650	0.8524	1.3388
	1.2256	1.1115	1.9633	1.0266	1.3016	1.7350	1.3015
Mean	3.3645	3.1777	4.6425	3.0332	3.5914	4.3219	
S.E.	2.5797	2.2968	3.1045	2.3837	2.5652	3.0214	
3%	1.0142	0.6803	1.3117	0.8244	0.08097	1.1839	1.6543
	1.0983	0.6965	1.3331	0.9548	0.8326	1.1738	1.9307
	2.5997	2.2457	3.7225	2.2241	2.5161	3.4531	1.9503
	9.6215	6.3487	9.9007	8.6788	7.5404	9.4376	1.9647
	13.1068	8.2403	11.6091	12.2323	9.2933	11.3693	2.1189
	1.1294	0.8699	1.5043	0.9051	0.9687	1.2210	1.2784
	6.4406	4.3256	7.1116	5.8032	5.6603	7.0795	2.3291
Mean	5.0015	3.3439	5.2133	4.5175	3.9459	4.9883	
S.E.	4.8478	3.0386	4.3347	4.5301	3.5330	4.2907	
4%	10.0288	6.3667	10.6383	8.9997	7.9969	9.8106	2.2230
	10.4799	6.2269	11.8377	9.1190	8.4675	10.6617	2.4678
	10.1882	7.4841	11.2654	9.2637	8.8112	10.7506	2.3627
	8.5368	4.4454	6.6681	7.8369	5.1617	6.4850	2.7851
	11.8171	5.6118	10.5594	10.3536	7.0551	9.7163	2.7887
	9.5618	5.0162	7.5657	8.8172	6.0662	7.0701	2.7997
Mean	10.1021	5.8585	9.7558	9.0646	7.2598	9.0824	
S.E.	1.0506	1.0774	2.1151	0.8096	1.4337	1.8442	
6%	14.6388	6.1601	9.6282	13.3602	7.6333	9.8061	3.8581
	3.9448	1.8244	3.1498	3.4445	2.3288	3.1064	3.6076
	20.6975	6.3246	9.7664	19.6311	7.2544	9.8581	4.7071
	5.9800	2.6582	5.3634	5.1135	3.5886	4.6372	3.3630
	23.2982	8.7590	12.7106	21.7470	10.0566	12.4544	4.2013
Mean	13.7119	5.1453	8.1237	12.6593	6.1723	7.9724	
S.E.	8.6130	2.8589	3.8197	8.2694	3.1560	3.9309	

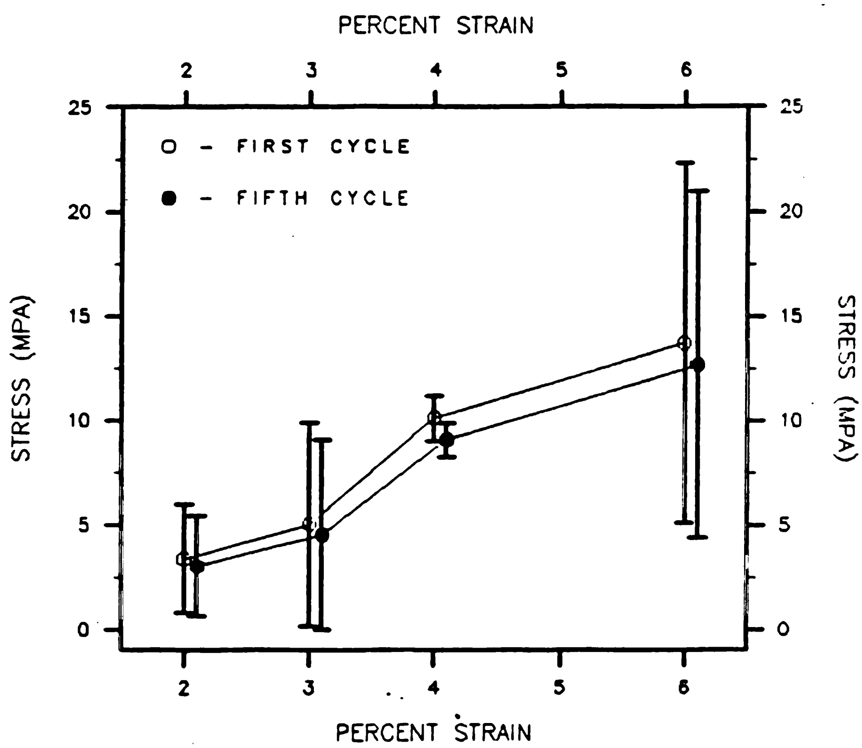

Figure 8 - Means for the peak stress for the first and fifth cycles at the strain levels tested.

TABLE 3 - Significant differences Between Strain Levels for the Peak Stress means, and the Loading and Unloading Maximum Tangent Moduli (M.T.M.) means for the First and Fifth Cycles*

	Strain Level Interval Tested**					
	6%-4%	6%-3%	6%-2%	4%-3%	4%-2%	3%-2%
Peak Stress						
1st cycle	N	N	Y	Y	Y	N
5th cycle	N	N	Y	Y	Y	N
Loading M.T.M.						
1st cycle	N	N	N	Y	Y	N
5th cycle	N	N	N	Y	Y	N
Unloading M.T.M.						
1st cycle	N	N	N	Y	Y	N
5th cycle	N	N	N	Y	Y	N

*Behrens-Fisher test (p=0.05) using Cochran and Cox estimates for the critical values [27].

**N indicates no significant differences, Y does.

meaningful. However, the statistical results clearly show a distinct significant rise in the mean peak stress with an increase in strain level. No known explanation could account for the much smaller scatter in the 4% tests. Means and standard errors of the cross-sectional areas and initial lengths, and the particular tendons used for these tests, were not substantially different from the other tests. In Table 4, repeated measures results between the first and fifth cycles indicate statistically significant decreases in the peak stress at all strain levels, indicating significant cyclic relaxation at all strain levels within the first five cycles.

TABLE 4 - Repeated Measures results for the Peak Stress, Loading and Unloading Maximum Tangent Moduli between the First and Fifth Cycles*

	Strain Level**			
	2%	3%	4%	6%
Peak Stress	Y	Y	Y	Y
Loading M.T.M.	Y	Y	Y	Y
Unloading M.T.M.	Y	Y	Y	N

*Tau-Test, one sided, p=0.05, see Ref. 25, p.44.
**N indicates no significant difference, Y does.

In Figure 9, a plot of the peak stresses-vs.-offset strain is shown. The offset strain is the strain level of the test minus the loading slack strain at the fifth cycle. The fifth cycle was chosen because it is thought that any gross initial changes in the tissue would have occured by this time. Hence, the scatter in the data may be reduced by accounting for variations in the initial changes in the samples, possibly caused by variations in the pretest condition of the samples (e.g. minor variations in hydration and sample mounting). In

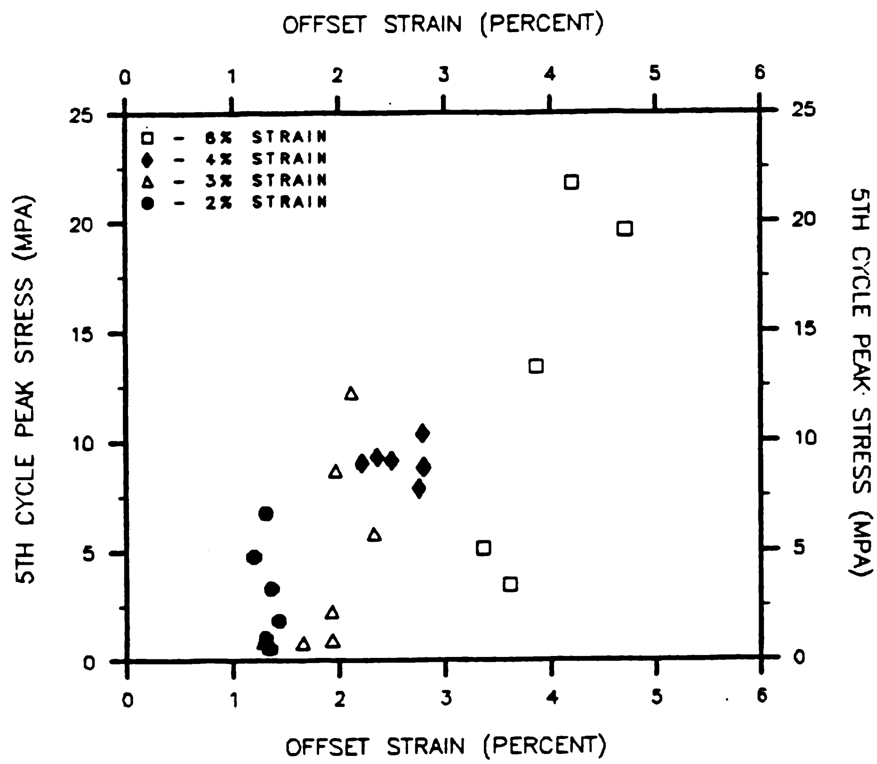

Figure 9 - The peak stresses-vs.-offset strain at the fifth cycle.

Figure 9, a large amount of scatter occurs in the data, however, certain trends are apparent. There appears to be a decrease in the range of the offset strain with a decrease in strain level. A linear regression was done on the data to check if the stress peaks correlated to the offset strain. The regresssion indicated a slope significantly different (p=0.005) from zero, and having a value of 4.67 MPa/%, showing a definite correlation. However, the scatter in the data cannot be solely accounted for by the pretest conditions of the samples, and appears to be due to either inherent differences in the mechanical response, slippage, or damage due to gripping.

Results for the stabilization times for the peak stress and Maximum Tangent Moduli (M.T.M.) are listed in Table 5. For the peak stress, results for the 1% difference criterion were eliminated because they were virtually identical to the t-test results (i.e., the significant difference was commonly 1% of the peak stress). In Figure 10, the stabilization times for the peak stress are plotted for all strain levels, for each criterion. Substantial differences for the stabilization times occur between the different criteria. Statistical results for the stabilization times of the peak stress, listed in Table 6, indicate no significant difference between strain levels for the t-test criterion. However, the 2% difference criterion showed that the 6% strain level was statistically different from the other strain levels; and the 5% criterion results indicate statistical differences occuring at the 6%-4% and 6%-2% intervals. No significant difference occured between either the 4 or 3 percent tests and the 2 percent tests for the 5% criterion; however, the 2% strain level appears to stabilize faster than the higher strain levels. Although

TABLE 5 - Stabilization Times (sec.) for the Peak Stress, and the Loading and Unloading Maximum Tangent Moduli*

Strain Level	t-test Criterion	S.E.	2% Criterion	S.E.	5% Criterion	S.E.
2%	7067	2188	5517	1818	1733	1329
3%	6300	2272	5357	2408	2871	2422
4%	7417	1234	4483	1982	2367	1371
6%	8260	594	7160	669	4600	1140

Strain Level	Loading t-test Criterion	M.T.M. S.E.	Unloading t-test Criterion	M.T.M. S.E.
2%	1317	1370	1400	1233
3%	2707	2653	4100	3122
4%	2400	2228	3417	1998
6%	7640	882	7580	1445

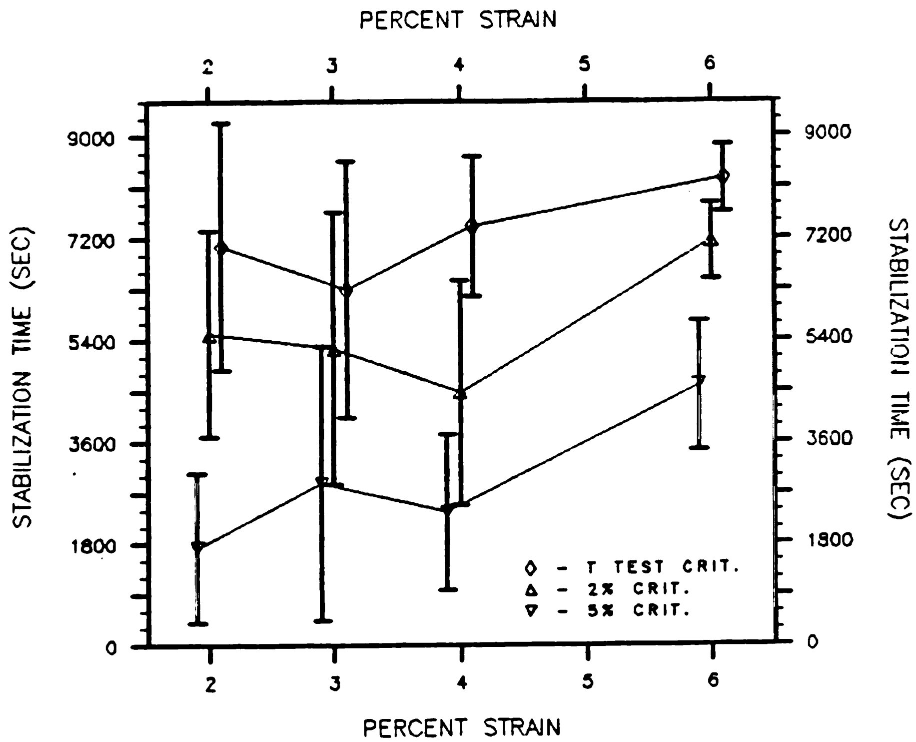

Figure 10 - Stabilization times for the peak stress.

TABLE 6 - Statistical differences of the Stabilization Times Between Strain Levels of the Peak Stress, and the Loading and Unloading Maximum Tangent Moduli*

	Strain Level Interval Tested**					
	6%-4%	6%-3%	6%-2%	4%-3%	4%-2%	3%-2%
Peak Stress						
t-test Criterion	N	N	N	N	N	N
2% Criterion	Y	Y	Y	N	N	N
5% Criterion	Y	N	Y	N	N	N
L-M.T.M.						
t-test Criterion	Y	Y	Y	N	N	N
U-M.T.M.						
t-test Criterion	Y	Y	Y	N	Y	Y

*Behrens-Fisher test (p=0.05) using Cochran and Cox estimates for the critical values [27].
**N indicates no significant difference, Y does.

the large scatter in the data makes conclusive trends from the statistical results difficult to obtain, there is an overall rise in stabilization time with an increase in strain level for the peak stress.

C. Loading and Unloading Maximum Tangent Moduli

Figure 11 shows a typical loading and unloading Maximum Tangent Moduli (M.T.M.)-vs.-time plot. In the loading M.T.M., an initial increase occurs, then a gradual decrease continues to the end of the test, similar to the behavior reported for human tendon [Hubbard-16]. The unloading M.T.M. decays rapidly at first, then continues to more slowly.

Figure 12 shows these curves plotted on semi-log axes. Similar to the peak stress behavior, a linear behavior does not occur, although the latter part of the data appears to become somewhat linear. Because of this non-linearity, no curve fitting was done on the M.T.M. data.

The results for the M.T.M. data are listed in Table 2. These results are comparable to human tendon [Hubbard-16], which have value of 6 MPa/% at 7%; strain and for primate [Selke, et. al.-28], which has a value of about 7.7 MPa/% at 5% strain. Figure 13 shows the loading M.T.M. means plotted against strain level for the 1st and 5th cycle. A sharp rise occurs at the 4%-3% interval, with the 6%-4% and 2%-3% intervals remaining relatively constant. The means at the fifth cycle are greater than the 1st cycle for all strain levels, with larger increases at higher strain levels.

Statistical differences for the loading M.T.M., listed in Table 3, occur only at the 4%-3% and 4%-2% intervals. An explanation for this could be that the 4 and 6 percent strain levels lie within

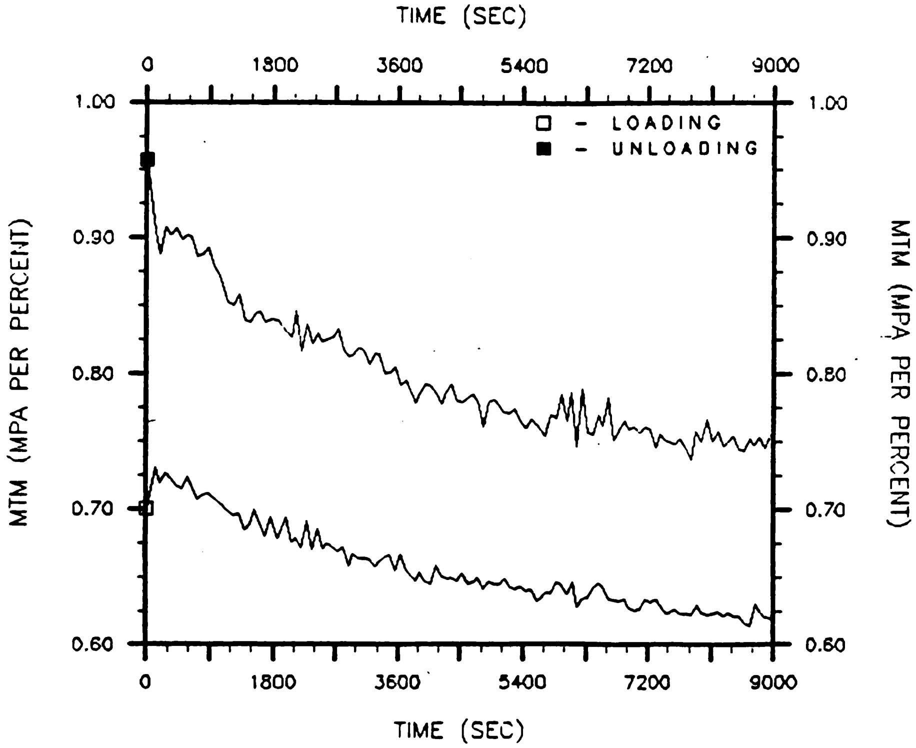

Figure 11 - A typical loading and unloading Maximum Tangent Moduli (M.T.M.)-vs.-time plot.

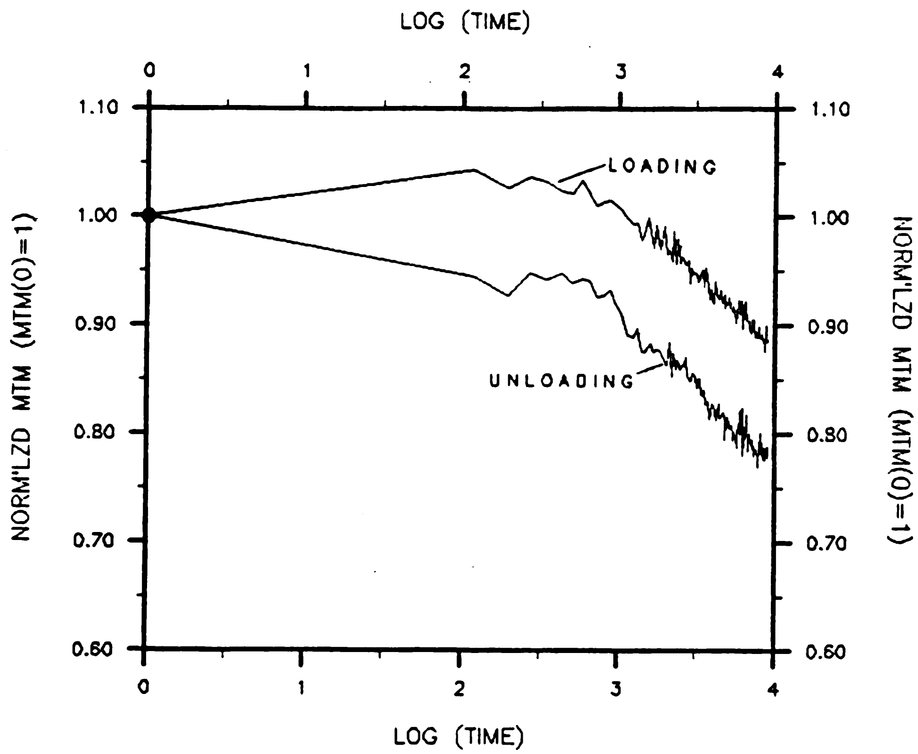

Figure 12 - A typical loading and unloading Maximum Tangent Moduli (M.T.M.)-vs.-log time plot.

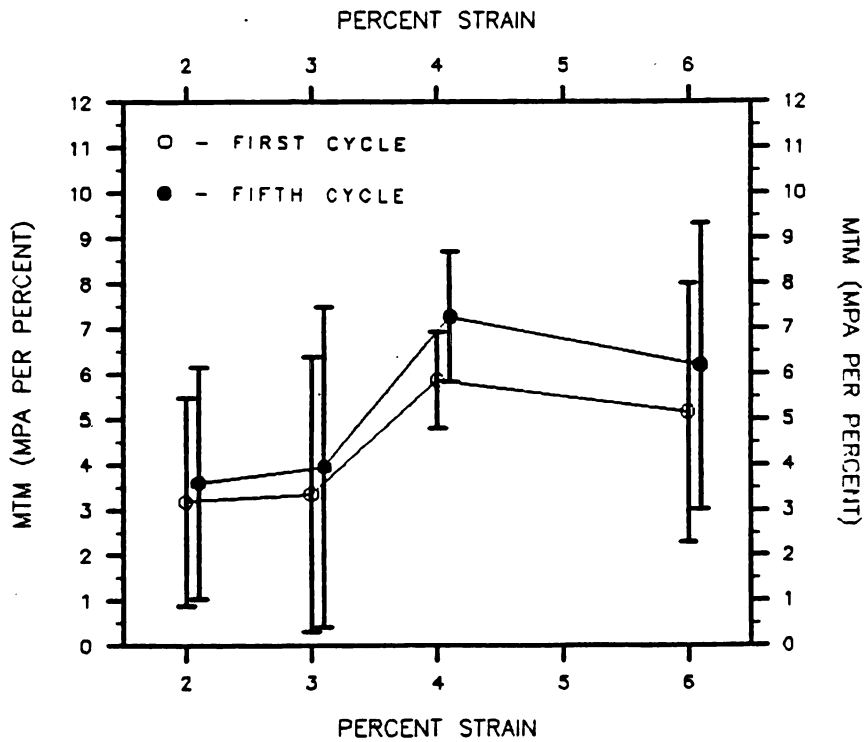

Figure 13 - The loading Maximum Tangent Moduli (M.T.M.)-vs.-strain level for the first and fifth cycles.

Region III, where a constant stiffness occurs. However, the occurance and precise definition of this region for these tests are beyond the present study. The lack of a statistical significant difference at the 3%-2% interval could be due to a lower signal-to-noise ratio for the load-deflection signals for 2% strain than those at 3% strain. The M.T.M. data are calculated from these signals, and a larger proportional error in the signals for 2% strain would induce a larger error in the M.T.M. data.

Repeated measures for the loading M.T.M. listed in Table 4, show significant increases between the 1st and 5th cycle for all strain levels. These results indicate substantial stiffening of the sample within the first five cycles at all strain levels tested.

Means for the unloading M.T.M. for both the 1st and 5th cycles are plotted in Figure 14. Again, a large increase in the mean value occurs at the 4%-3% interval at both cycles. Also a decrease in the means can be seen at all strain levels from the first to the fifth cycles. Statistical results, taken from Table 3, indicate significant differences occur only at the 4%-3% and 4%-2% intervals. The significant differences occuring only at these intervals could be explained by a lower signal-to-noise ratio at 2% strain as proposed for the loading M.T.M.

Repeated measures results for the unloading M.T.M., listed in Table 4, indicate significant differences between the 1st and 5th cycles occuring at the 2%, 3%, and 4% strain levels. Precisely why the 6% unloading M.T.M. does not change significantly from the first to the fifth cycle is not known. It is possible that the same mechanisms previously mentioned that caused a lower peak stress also

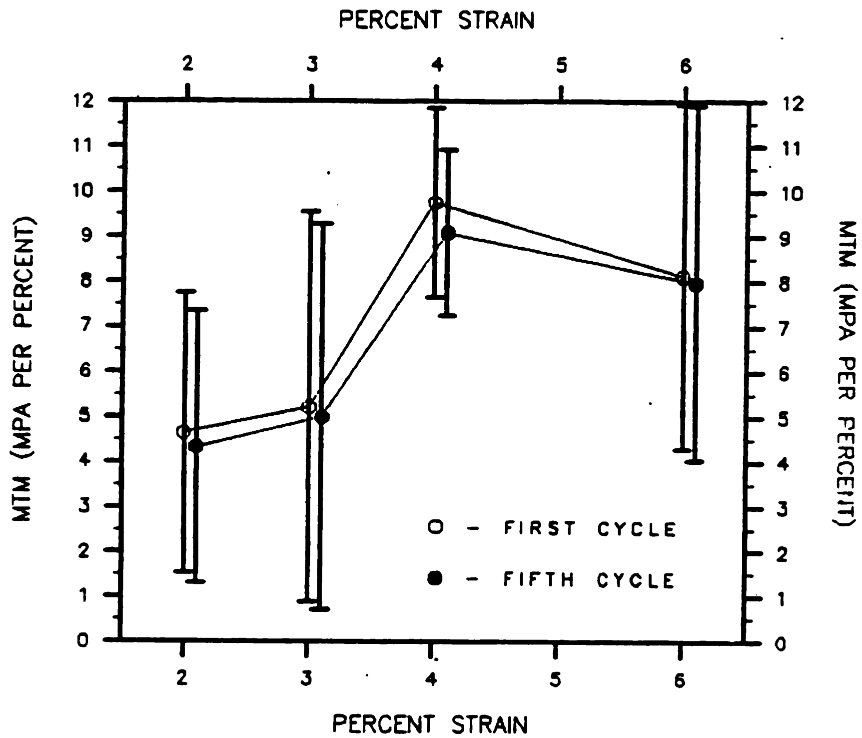

Figure 14 - The unloading Maximum Tangent Moduli (M.T.M.)-vs.-strain level for the first and fifth cycles.

cause the unloading M.T.M. to remain relatively constant between 4% and 6% strain.

In Figures 15 and 16 the loading and unloading M.T.M., respectively, are plotted against the offset strain at 5th cycle taken from Table 2. The overall trend is very similar to the peak stress response; a decrease in the range of the offset strain occurs with a decrease in strain level. The similarity is mostly due to the fact that the offset strain values are identical in all the offset plots. A linear regression on both the loading and unloading M.T.M. indicates that the slopes are statistically different from zero, showing a definite increase in both loading and unloading M.T.M. with an increase in strain level. Similar to the peak stress data, plotting against the offset strain does not reduce the scatter, implying that variations in pretest conditions does not fully account for the scatter in the M.T.M. data.

Stabilization times for the M.T.M. are listed in Table 5, and are shown in Figure 17. The results for the 1%, 2%, and 5% difference criteria were eliminated because of noise in the M.T.M.-versus-time curves; generally a difference of about 5% was needed for a statistical significance. The t-tests results indicate a rise in stabilization time with an increase in strain level. Also, the unloading M.T.M. appears to take longer to stabilize than the loading M.T.M. Statistical results, listed in Table 6, indicate that only at the 6% strain level are loading M.T.M. results significantly different from the other strain levels. The unloading data indicate that both the 6% and 2% tests are different from the other strain levels. The large data scatter in the M.T.M. data probably masks the more subtle

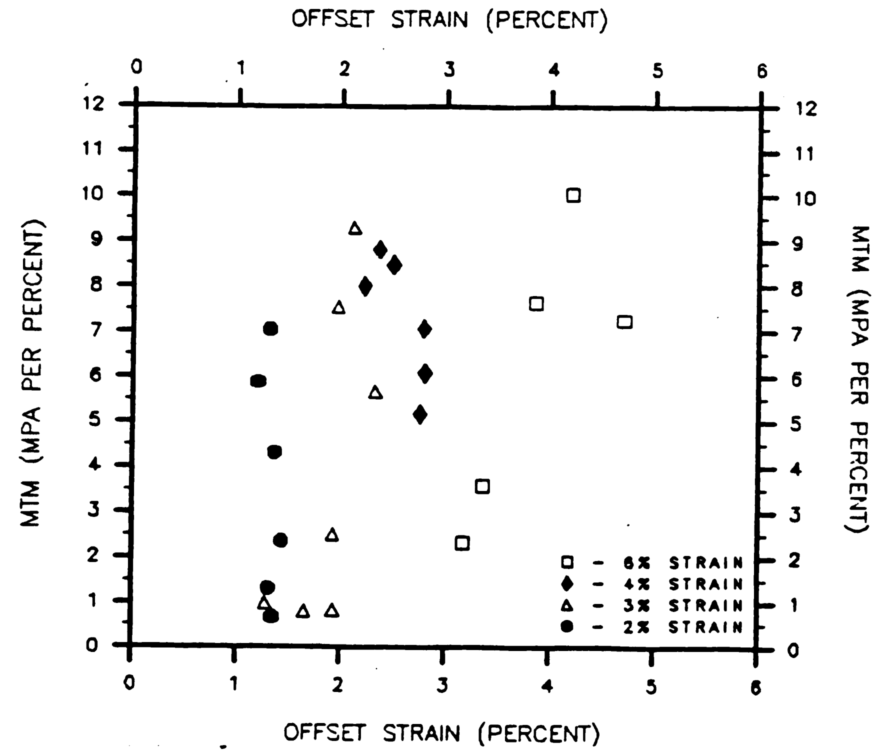

Figure 15 - Loading Maximum Tangent Moduli (M.T.M.)-vs.-offset strain at the fifth cycle.

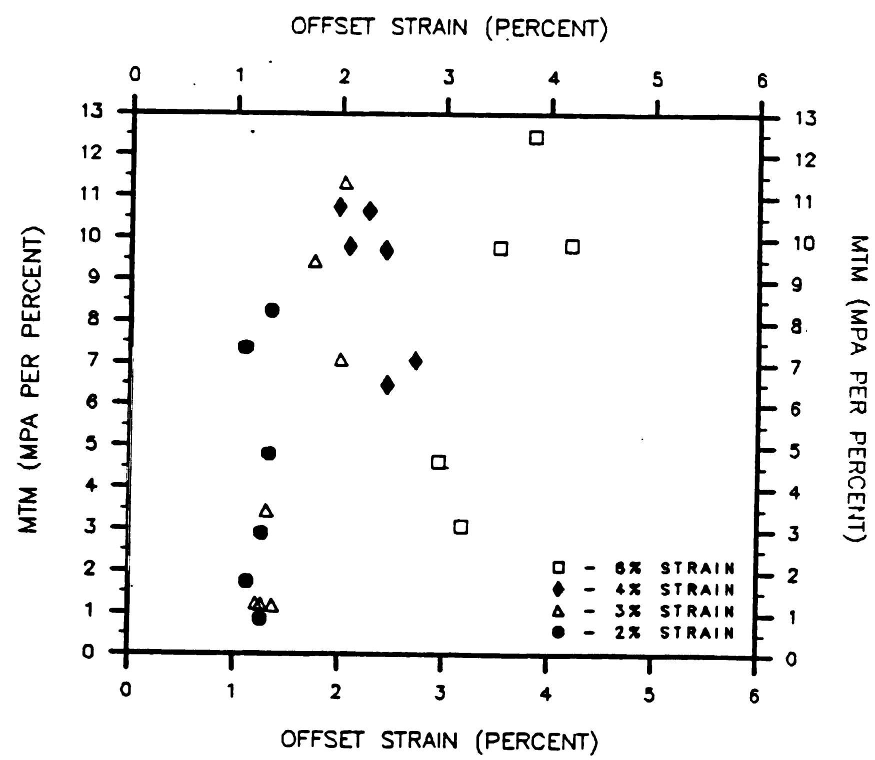

Figure 16 - Unloading Maximum Tangent Moduli (M.T.M.)-vs.-offset strain at the fifth cycle.

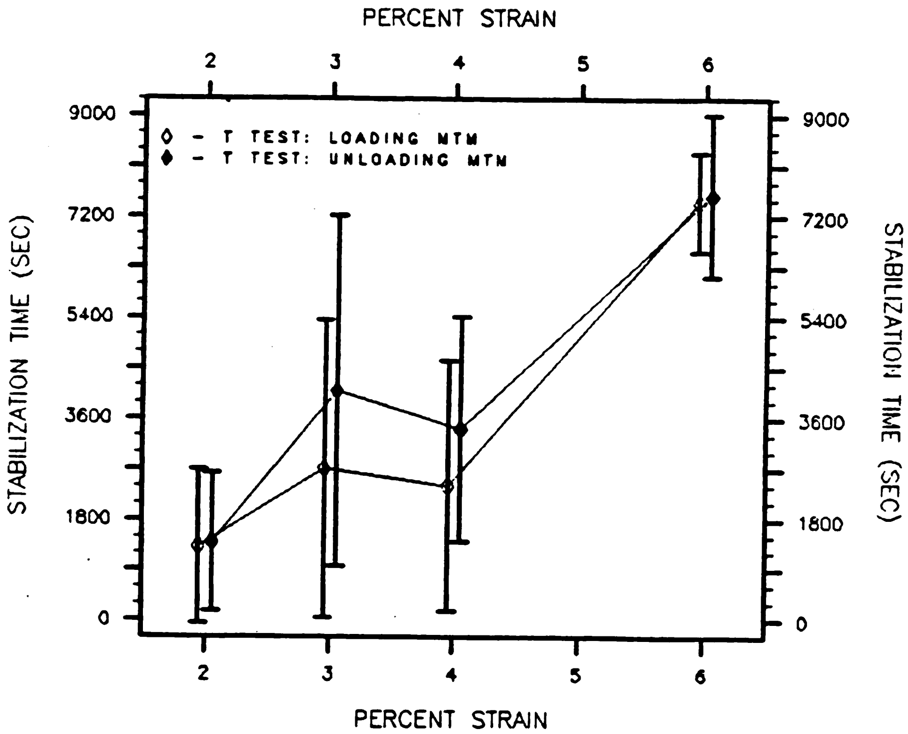

Figure 17 - Stabilization times for the loading and unloading Maximum Tangent Moduli (M.T.M.).

trends in the data. However, the above results imply a significant rise in stabilization time at 6% strain for the loading M.T.M., and an overall significant rise in stabilization time with an increase in strain level for the unloading M.T.M.

D. Hysteresis

Results for the hysteresis data are listed in Table 7. Figures 18-21 shows these values plotted for the initial response (the first data group, corresponding to the initial 12 seconds of the test) for the 2%, 3%, 4%, and 6% strain levels, respectively. These results are comparable to human values of 15% - 45% [Hubbard-16], and to primate 19% - 38% [Selke, et. al.-27]. For all strain levels, a rapid initial decrease occurs, with slower changes at the end of the data group. The initial hystersis ranged at 40%-47%, then droped to about 17%-22% after 12 seconds for all strain levels. Repeated measures for the hysteresis data, listed in Table 8, indicate significant decreases occur throughout all strain levels during the initial 12 seconds of testing.

Figures 22-25 are plots of the long term response for the hysteresis for the 2%, 3%, 4%, and 6% tests, repectively. The first and last cycles in the first data group are shown on these plots as coinciding. All strain levels show a sharp decrease between the last cycle in the first data group and the cycle at 1800s, and approach a value of about 17% by 9000s. Repeated measures for the hysteresis, listed in Table 8, reveal that significant changes occur between 12s and 1800s, but almost no significant changes after 1800s. It appears that significant changes in the hysteresis occur only in the initial 1800s. A future investigation of the initial 1800s would be necessary

TABLE 7 - Hystersis Data (%)

	Cycle #1	Cycle #2	Cycle #3	Cycle #5	12s	1800s	3600s	5400s	7200s	9000s
2%										
Mean	42.93	27.14	25.75	25.13	22.33	17.78	19.04	18.19	17.33	17.33
S.E.	8.42	5.35	6.36	5.69	5.10	3.43	5.32	3.90	4.38	4.29
3%										
Mean	47.35	31.03	28.00	26.01	23.76	20.86	20.92	19.85	20.40	20.65
S.E.	9.41	8.69	7.88	7.59	6.29	6.56	7.77	5.72	6.35	8.33
4%										
Mean	42.27	23.53	21.16	19.66	18.61	15.32	14.64	14.92	14.95	15.00
S.E.	7.72	4.12	3.82	3.45	3.08	2.83	3.03	2.38	3.23	2.71
6%										
Mean	39.85	21.29	19.57	18.16	+	14.61	14.33	13.97	13.74	14.56
S.E.	8.87	3.91	4.04	3.77	+	2.85	2.63	2.68	2.15	2.04

+For the 6% strain level tests, the fifth cycle occurs at 12s.

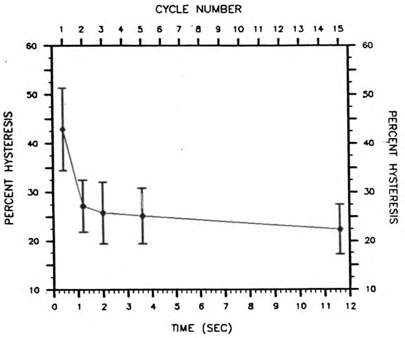

Figure 18 - The initial response of the hysteresis at the 2% strain level.

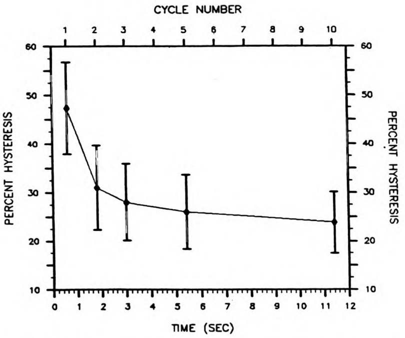

Figure 19 - The initial response of the hysteresis at the 3% strain level.

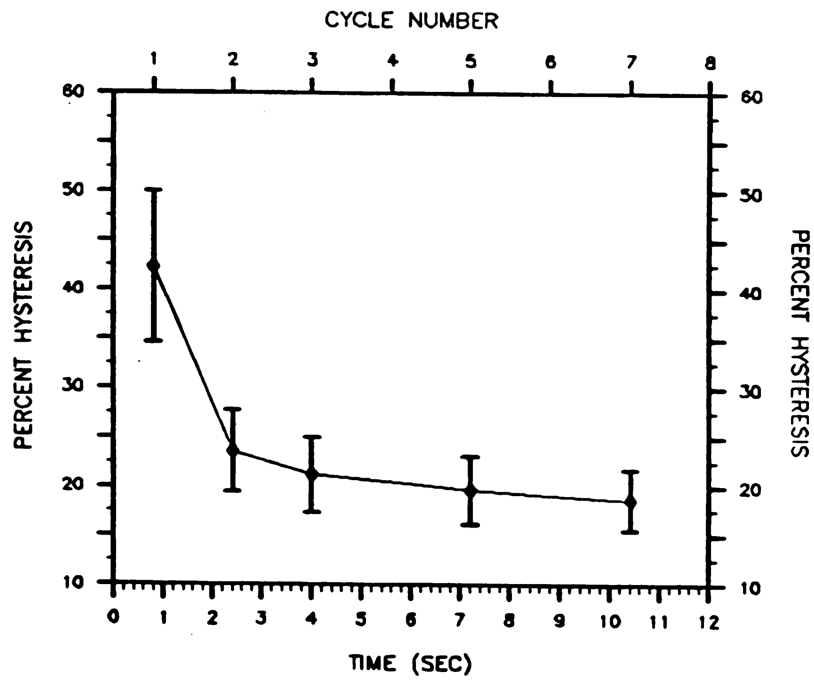

Figure 20 - The initial response of the hysteresis at the 4% strain level.

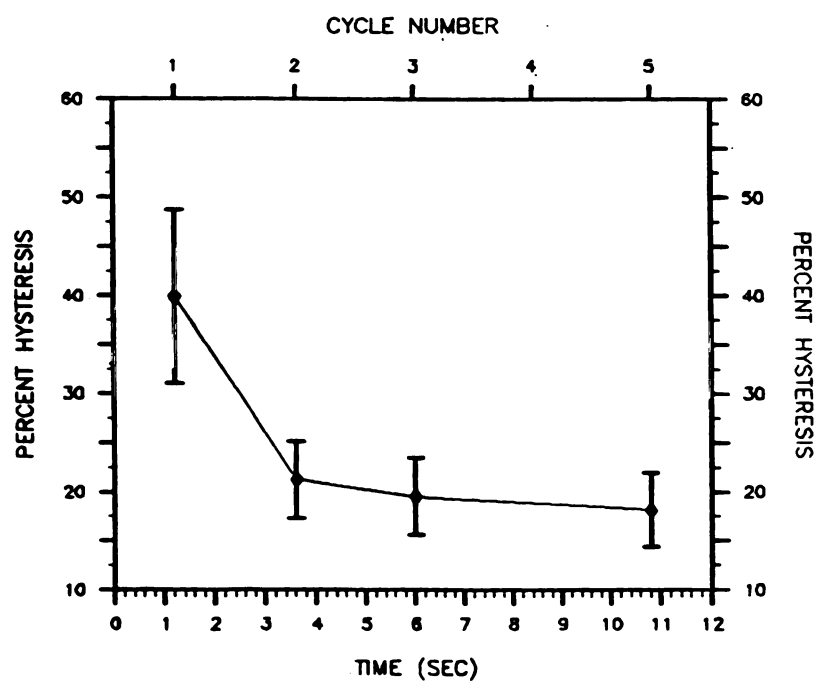

Figure 21 - The initial response of the hysteresis at the 6% strain level.

TABLE 8 - Repeated Measures for the Hysteresis*

	Cycles 1-2	Cycles 2-3	Cycles 3-5	Cycle 5 - 12s	12s -1800s	1800s -3600s	3600s -5400s	5400s -7200s	7200s -9000s	1800s -9000s	12s -9000s
2%	Y	Y	Y	Y	Y	N	N	N	N	N	Y
3%	Y	Y	Y	Y	Y	N	N	N	N	N	N
4%	Y	Y	Y	Y	Y	Y	N	N	N	Y	Y
6%	Y	Y	Y	-	Y	N	N	N	N	N	Y

*Tau-test, $p=0.05$, N indicates no significant difference, Y does.
+For the 6% strain level tests, the fifth cycle occurs at 12s.

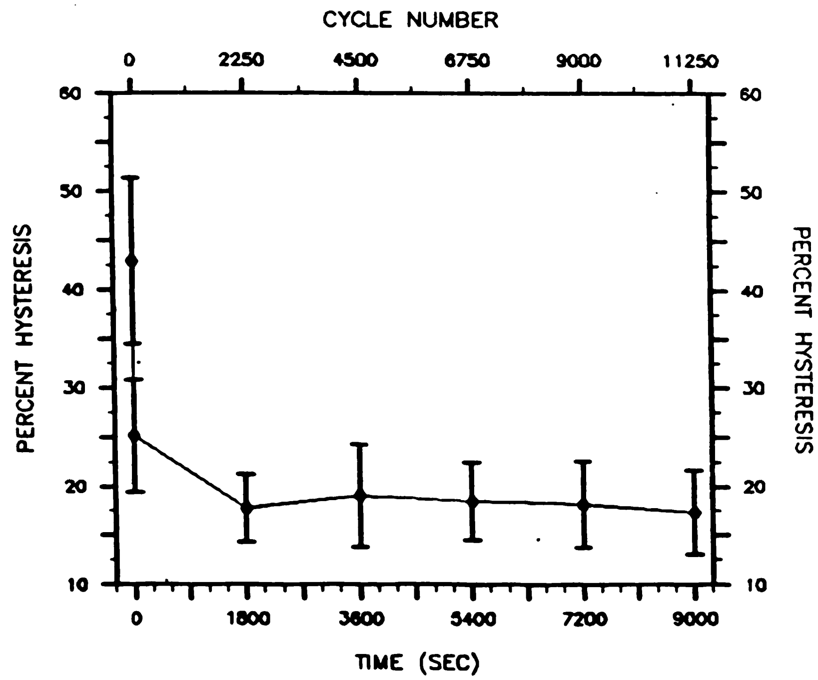

Figure 22 - The long term response of the hysteresis at the 2% strain level.

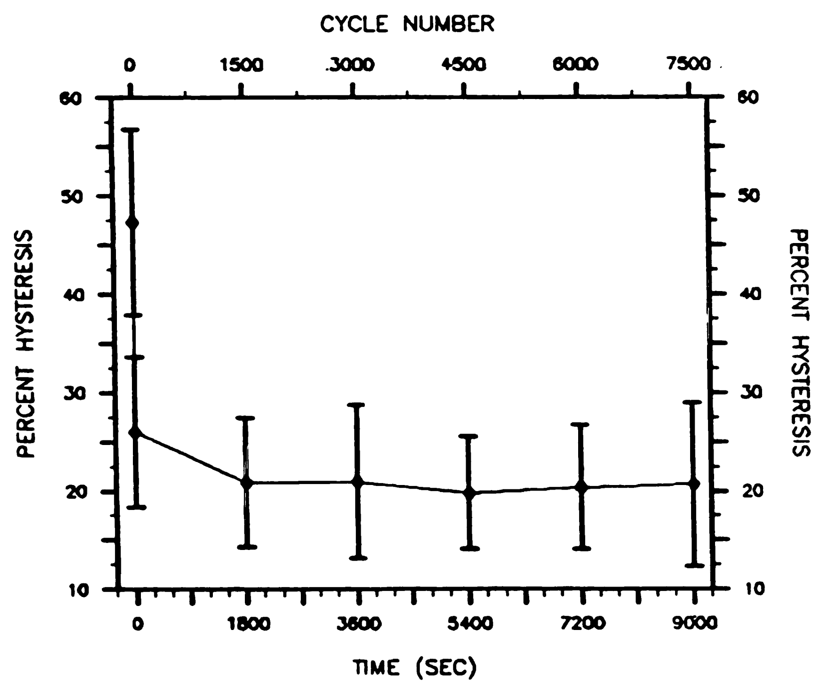

Figure 23 - The long term response of the hysteresis at the 3% strain level.

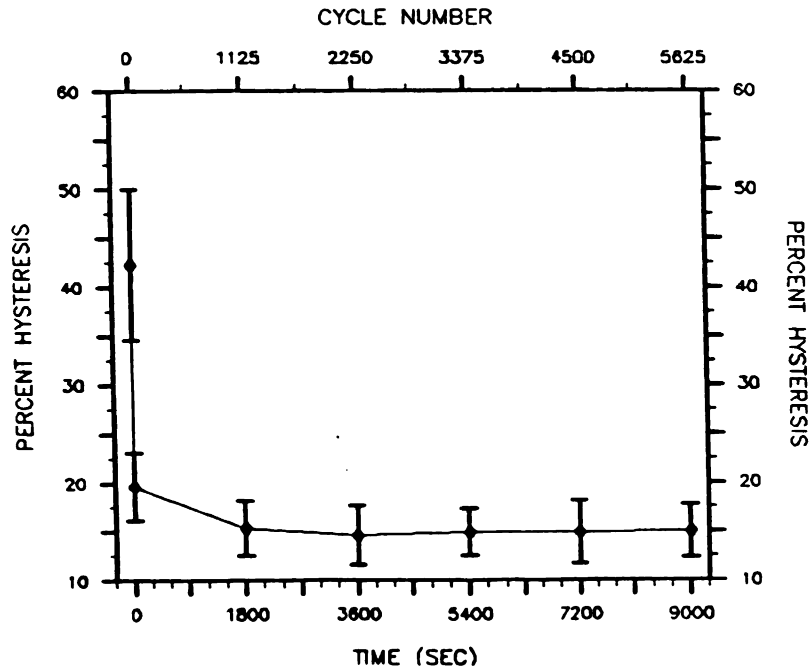

Figure 24 - The long term response of the hysteresis at the 4% strain level.

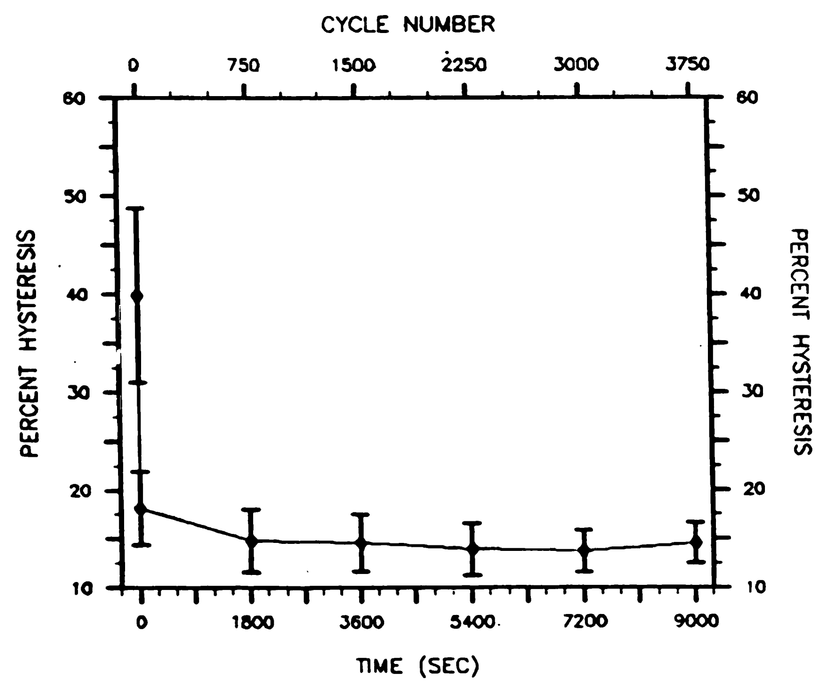

Figure 25 - The long term response of the hysteresis at the 6% strain level.

to determine more precisely when the hystersis stabilizes within the initial 1800s. Statistical results for differences between strain levels for the hysteresis, listed in Table 9, indicate almost no significant difference between strain levels. Scatter may be masking out very small differences in hysteresis between strain levels, but present results imply the hysteresis behavior is essentially insensitive to strain level.

TABLE 9 - Significant differences Between Strain Levels for the Hysteresis*

	Strain Level Interval Tested**					
	6%-4%	6%-3%	6%-2%	4%-3%	4%-2%	3%-2%
1st Cycle	N	N	N	N	N	N
Last Cycle	N	N	N	N	N	N
1800s	N	Y	N	Y	N	N
3600s	N	Y	N	Y	N	N
9000s	N	N	N	N	N	N

*Behren-Fisher test (p=0.05) using Cochran and Cox estimates for the critical values [27].
**N indicates no significant difference, Y does.

E. Slack Strain

Table 10 lists the loading and unloading slack strain results for all strain levels. The initial loading slack strains are zero by definition; the sample being at its initial length at the beginning of the test. Figures 26-29 show the initial responses (first 12 sec. of the test) of the slack strain at the 2%, 3%, 4%, and 6% strain levels, respectively. A general trend at all strain levels is that the differences between the loading and unloading data diminish with time. Also, succesive increases in the slack strain decrease with time. Figures 30-33 show the long term responses of the slack strain at the

TABLE 10 - Results for the Slack Strain (%)

	Cycle #1	Cycle #2	Cycle #3	Cycle #5	12s	1800s	3600s	5400s	7200s	9000s
2%										
Loading										
Mean	0.000	0.7375	0.6779	0.6787	0.7759	0.9068	1.0180	1.012	1.0650	1.0530
S.E.	0.000	0.0541	0.0571	0.0770	0.1235	0.1682	0.1278	0.2022	0.1985	0.1793
Unloading										
Mean	0.7562	0.7559	0.7723	0.7703	0.9941	1.0650	1.0870	1.1600	1.1320	1.1890
S.E.	0.1767	0.1347	0.1976	0.1026	0.3276	0.2257	0.1656	0.1514	0.1402	0.1830
3%										
Loading										
Mean	0.0000	0.9424	1.0313	1.1130	1.2030	1.4825	1.6458	1.7304	1.7350	1.7150
S.E.	0.0000	0.3155	0.2580	0.3375	0.3251	0.2620	0.2609	0.2483	0.2555	0.2628
Unloading										
Mean	1.1765	1.2670	1.3870	1.4400	1.4780	1.7680	1.8060	1.8740	1.8540	1.8310
S.E.	0.4056	0.3979	0.3634	0.3571	0.3543	0.3179	0.3640	0.3370	0.2011	0.3143
4%										
Loading										
Mean	0.0000	1.2299	1.3284	1.4284	1.5210	2.0398	2.0980	2.1107	2.1332	2.2328
S.E.	0.0000	0.1817	0.2850	0.2470	.03193	0.3613	0.4019	0.3456	0.3924	0.3142
Unloading										
Mean	1.5270	1.5604	1.6246	1.6817	1.7278	2.1844	2.2437	2.3386	2.3428	2.3668
S.E.	0.3027	0.2450	0.1789	0.2710	0.2777	0.3962	0.3775	0.3794	0.4068	0.3898
6%										
Loading										
Mean	0.0000	1.7045	1.8084	2.0526	+	2.9236	3.0119	2.9797	3.1861	3.2488
S.E.	0.0000	1.4644	0.6113	0.5260	+	0.6142	0.6756	0.6382	0.6172	0.6942
Unloading										
Mean	2.112	2.2889	2.3606	2.4605	+	3.1179	3.2409	3.3060	3.4045	3.4231
S.E.	0.5625	0.6087	0.6702	0.5057	+	0.6864	0.6754	0.6528	0.6031	0.6126

+For the 6% strain level tests, the fifth cycle occurs at 12s.

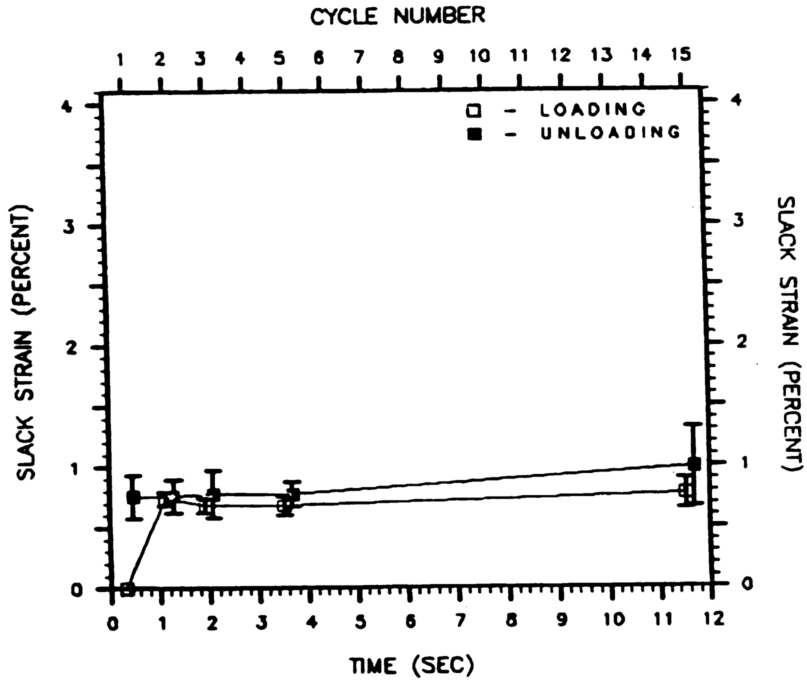

Figure 26 - The initial response of the slack strain at the 2% strain level.

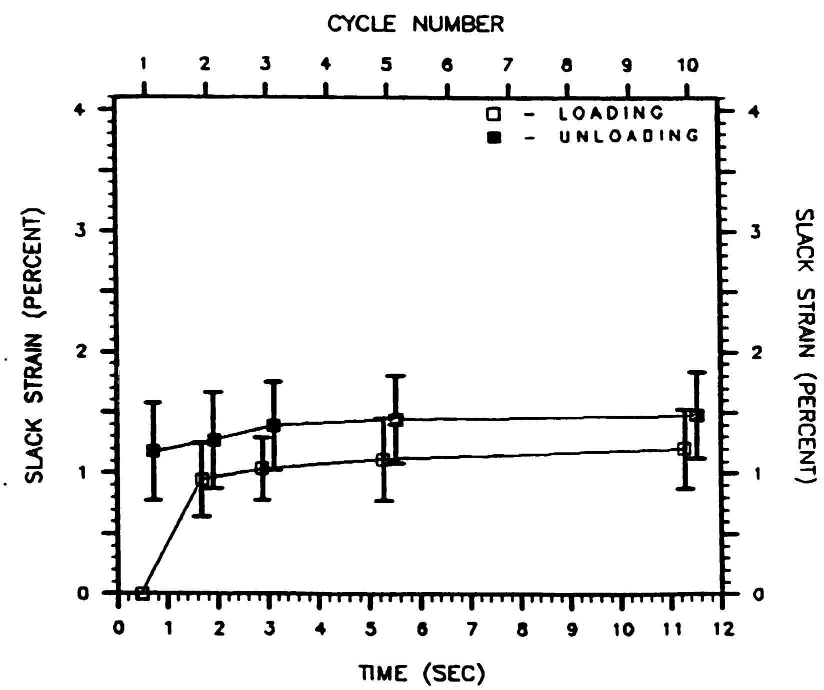

Figure 27 - The initial response of the slack strain at the 3% strain level.

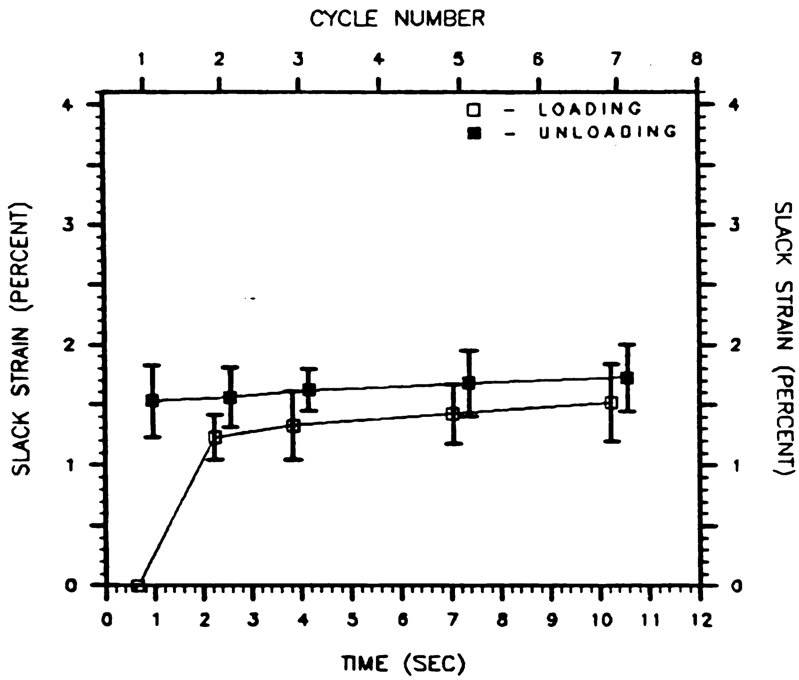

Figure 28 - The initial response of the slack strain at the 4% strain level.

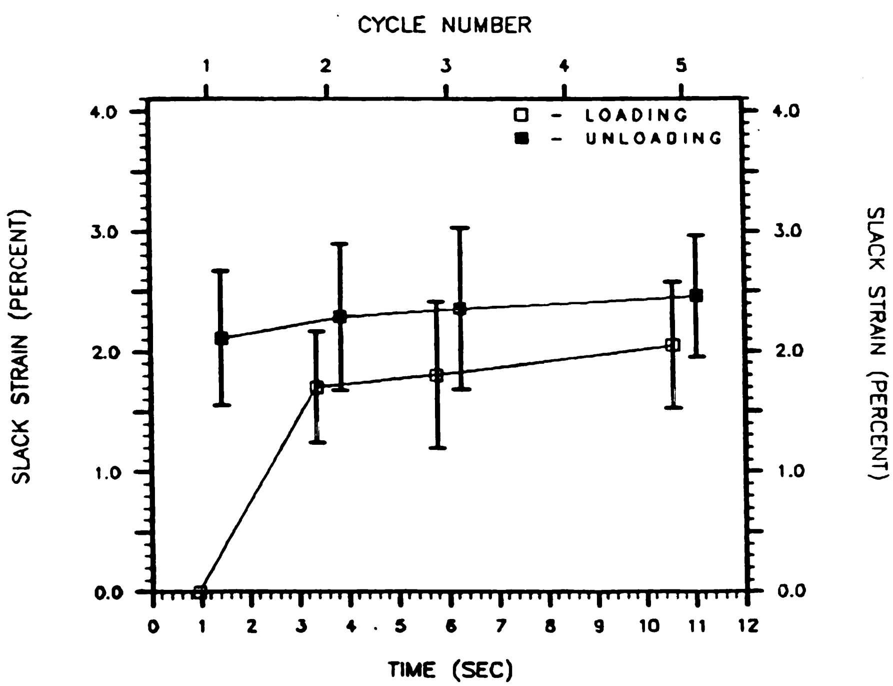

Figure 29 - The initial response of the slack strain at the 6% strain level.

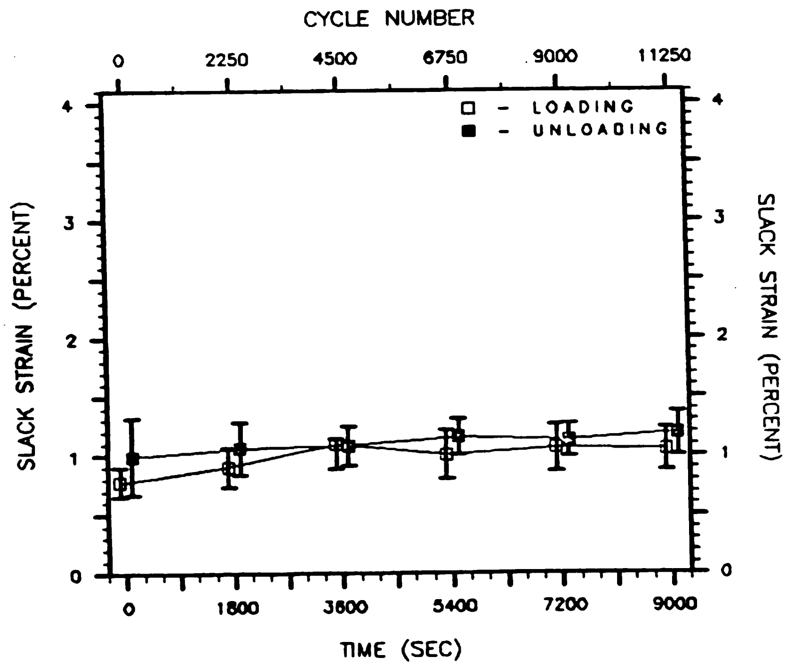

Figure 30 - The long term response of the slack strain at the 2% strain level.

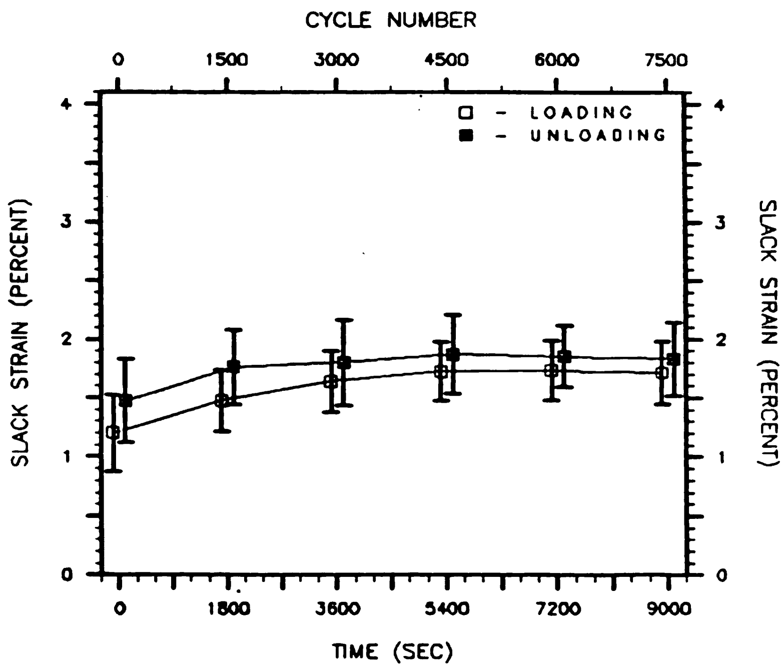

Figure 31 - The long term response of the slack strain at the 3% strain level.

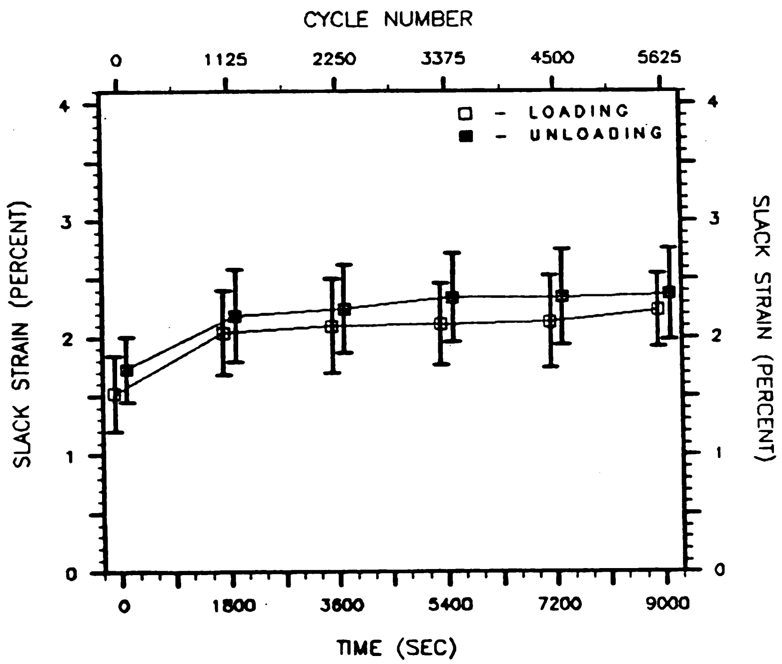

Figure 32 - The long term response of the slack strain at the 4% strain level.

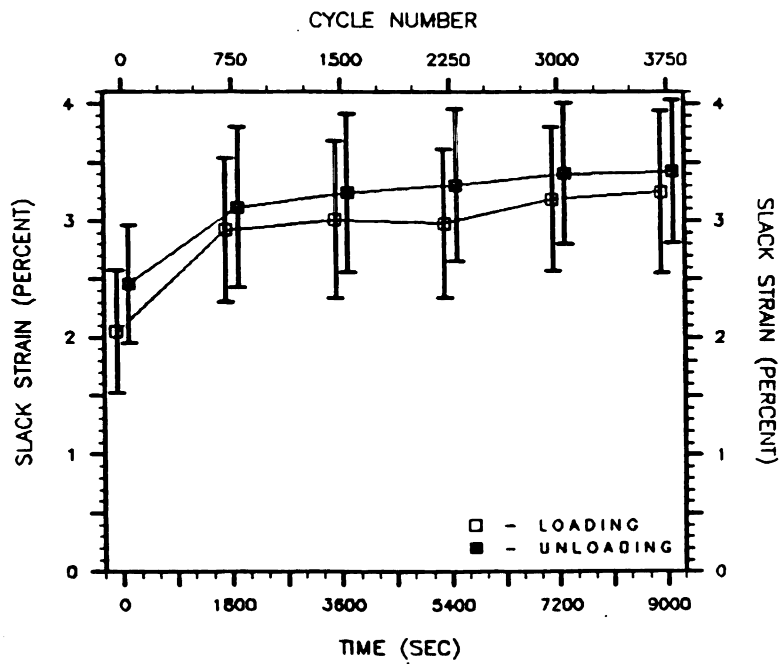

Figure 33 - The long term response of the slack strain at the 6% strain level.

2%, 3%, 4%, and 6% strain levels, respectively. In these plots, the first data points are the values for the last cycle in the first data group at 12s. The differences between the long term loading and unloading data appear to remain relatively constant. The largest increases occur between 12s and 1800s. Differences between strain levels can be more easily perceived in Figure 34, where the long term responses have been plotted for all strain levels together (standard errors have been removed for clarity). The greater increase in the loading and unloading slack strain between 12s and 1800s with an increase in strain level can be clearly seen. Also, there is an apparent greater rise in the slack strain past 1800s with an increase in strain level.

Statistics on the slack strain results are listed in Table 11. Generally, significant differences in the slack strain occur at all intervals, with a few inconsistent exceptions. These exceptions may be primarily due to data scatter, rather then indicating trends in the data. Repeated measures for the slack strain, listed in Table 12, indicate that statistical changes for the loading slack strain occur from 12s to 1800s for all strain levels; with the exception of the 2% tests, which occurs from 1800s-3600s. All unloading slack strain data show significant changes from 12s to 1800s. Generally, long term increases in the slack strain (both loading and unloading) are small enough that subsequent intervals past 1800s show no significant changes. However, all strain levels show significant changes both from 1800s to 9000s and from 12s to 9000s indicating significant increases occuring over these time periods. Interestingly, the 6% strain level shows several significantly different intervals past

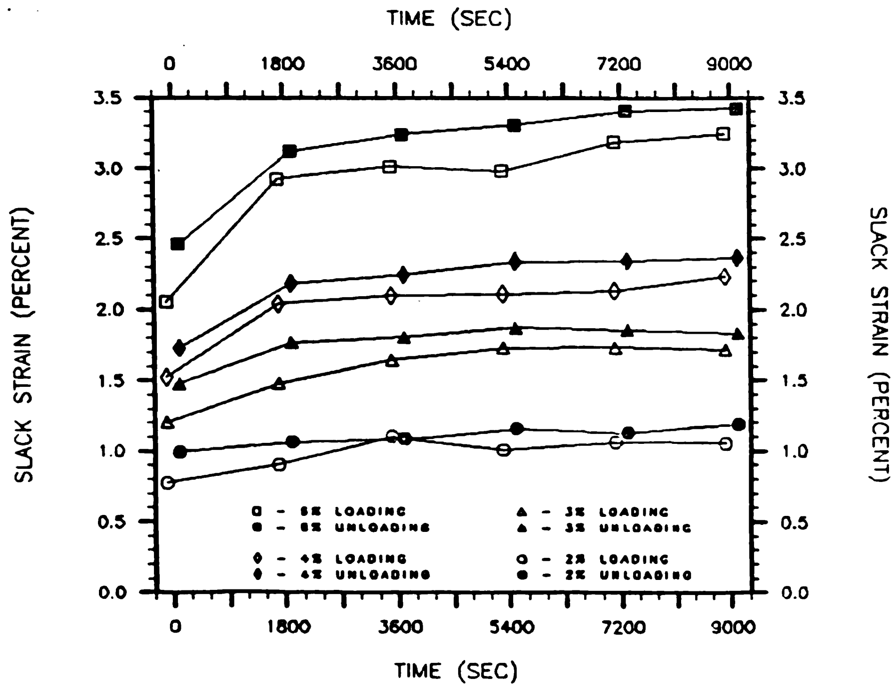

Figure 34 - The long term response of the slack strain for all strain levels (standard errors have been removed for clarity).

TABLE 11 - Significant differences Between Strain Levels for the Slack Strain*

	Strain Level Interval Tested**					
	6%-4%	6%-3%	6%-2%	4%-3%	4%-2%	3%-2%
<u>Loading</u>						
Last Cycle	N	Y	Y	N	Y	Y
1800s	Y	Y	Y	Y	Y	Y
3600s	Y	Y	Y	Y	Y	Y
9000s	Y	Y	Y	Y	Y	Y
<u>UnLoading</u>						
1st Cycle	N	Y	Y	N	Y	Y
Last Cycle	N	Y	Y	Y	Y	Y
1800s	Y	Y	Y	Y	Y	Y
3600s	Y	Y	Y	Y	Y	Y
9000s	Y	Y	Y	Y	Y	Y

*Behren-Fisher test ($p=0.05$) using Cochran and Cox estimates for the critical values [27]. Loading first cycle is always 2% so inclusion is unnecessary.

**N indicates no significant difference, Y does.

TABLE 12 - Repeated Measures for the Slack Strain*

	Cycles 1-2	Cycles 2-3	Cycles 3-5	Cycle 5 12s	12s -1800s	1800s -3600s	3600s -5400s	5400s -7200s	7200s -9000s	1800s -9000s	12s -9000s
<u>Loading</u>											
2%	Y	N	N	N	N	Y	N	N	N	Y	Y
3%	Y	N	N	N	Y	N	N	N	N	Y	Y
4%	Y	N	Y	N	Y	N	N	N	N	Y	Y
6%	Y	N	N	+	Y	N	N	N	N	Y	Y
<u>Unloading</u>											
2%	N	N	N	N	Y	N	N	N	N	N	Y
3%	Y	N	N	N	Y	N	Y	N	N	Y	Y
4%	N	N	N	N	Y	Y	Y	N	N	Y	Y
6%	N	N	N	+	Y	N	N	N	N	N	Y

*Tau-test, $p=0.05$
+For the 6% strain level tests, the fifth cycle occurs at 12s.

1800s, implying that changes at this level are larger than at the lower strain levels.

In Table 13 the mean proportional ranges of the slack strain are listed, and were calculated as the total increase in a mean value for a parameter over a specified interval divided by the strain level, then multiplied by 100 to express it in percent. This was done to see if the slack strain behavior was proportionally equal at all strain levels. The total mean proportional ranges for the loading slack strain are all close to 55%, and for the unloading data close to 22%. The increase from the first cycle to 12s is always about 38% for the loading data, but rises with strain level for the unloading data. Both the loading and unloading mean proportional ranges increase with an increase in strain level from 12s to 1800s. From 1800s to 9000s the loading and unloading slack strain mean proportional range appears to generally decrease with an increase in strain level. Larger increases occur for both the loading and unloading data from 12s to 1800s at higher strain levels. The initial responses (1st cycle to 12s) are approximately equal at all strain levels for the loading data, but generally increase with strain level for the unloading data. Finally, the decrease in the mean proportional range with an increase in strain level from 1800s to 9000s appears to "offset" the increase in the mean proportional range within an increase in strain level from 12s to 1800s (particularly in the loading data), which appears to help make the total ranges equal between strain levels. Generally, the total changes of the loading and unloading slack strain from the 1st cycle to 9000s are proportionally equal at the strain levels tested,

TABLE 13 - Mean Proportional Ranges of the Slack Strain (%)

Loading

Strain Level	1st Cycle-9000s	1st Cycle-12s	12s-1800s	1800s-9000s
2%	53.25	34.21	6.55	7.31
3%	57.17	38.03	9.32	7.75
4%	55.82	40.10	12.94	4.83
6%	54.08	38.80	14.52	5.35

Unloading

Strain Level	1st Cycle-9000s	1st Cycle-12s	12s-1800s	1800s-9000s
2%	21.64	5.80	3.55	6.20
3%	21.82	5.02	7.25	1.58
4%	21.00	10.05	11.42	4.56
6%	21.82	11.90	10.96	5.07

with the major increases in slack strain occuring in the initial 1800s.

F. Power Fit Coefficients

The power fits showed a high correlation to the data, with the correlation coefficient, r^2, attaining value of 0.95 or greater. Figure 35 shows a typical plot of the actual data plotted on log-log axis, with the fitted curve superimposed over it. Clearly, the data showed a marked linearity when plotted this way. In Figure 36, the identical data is shown plotted on normal linear axis, again showing the closeness of that fit.

Results for the power fit coefficient A are listed in Table 14. Figures 37-40 show the coefficient A plotted for the 2%, 3%, 4%, and 6% strain levels, respectively, for the first 12s of the test. Large scatter can be seen at all strain levels. The coefficient A acts as a scale factor in the regression fitting; and it appears to absorb most of the scatter in the data, as seen in the peak stress-vs.-offset strain plot (Figure 9). Overall (A) remains relatively constant in the initial part of the test. Figures 41-44 show the long term response of A for 2%, 3%, 4%, and 6% strain levels, respectively. Similar behavior is seen, with the A's remaining relatively constant throughout the test. Statistics for A, listed in Table 15 show no significiant differences occur at any interval, with only one exception, at the 6%-4% interval at 9000s. Repeated measures for A listed in Table 16, also yield identical results. The statistical results indicate that values for A are not different both within any strain level and between strain levels.

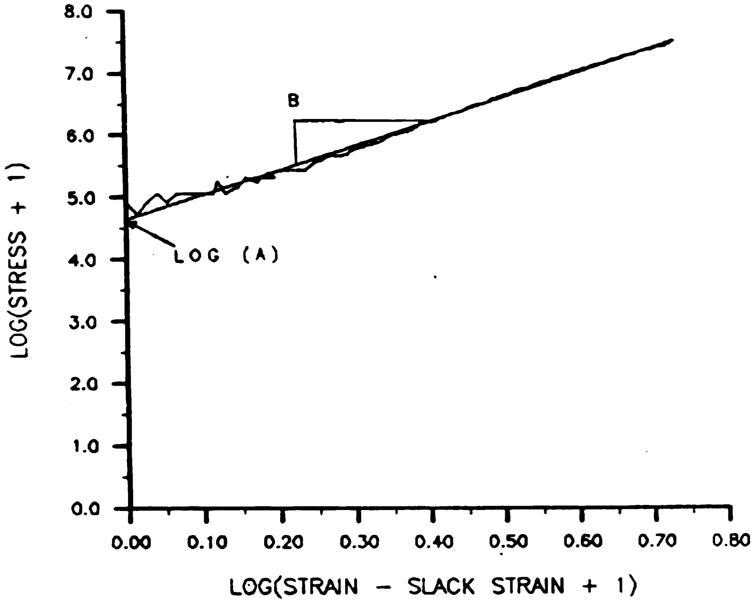

Figure 35 - A typical plot of a stress-strain curve plotted on log - log axes, with the fitted curve.

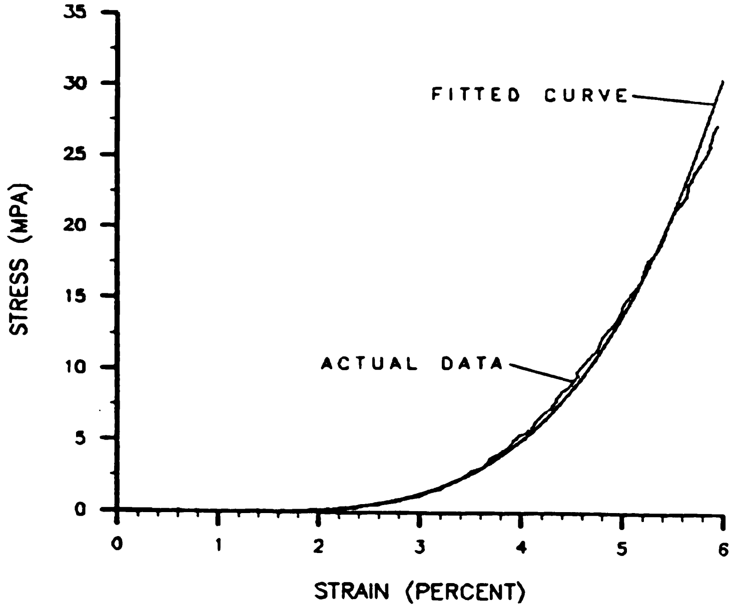

Figure 36 - A typical plot of a stress-strain curve plotted on linear axes, with the fitted curve.

TABLE 14 - A Results - Mean Values (in MPa x 10^{-5})

	Cycle #1	Cycle #2	Cycle #3	Cycle #5	12s	1800s	3600s	5400s	7200s	9000s
2%										
Loading										
Mean	0.3137	1.4293	0.8253	0.8129	0.6839	0.3658	0.4653	0.4131	0.4943	0.4033
S.E.	0.1882	1.2483	0.6331	0.8306	0.5729	0.3411	0.3101	0.3309	0.3183	0.2021
Unloading										
Mean	0.5292	0.4827	0.4083	0.3802	0.4271	0.4607	0.3299	0.2629	0.4512	0.5758
S.E.	0.5096	0.4253	0.1974	0.2575	0.0939	0.3393	0.1879	0.1512	0.3325	0.3977
3%										
Loading										
Mean	0.4920	0.6533	0.5742	0.6669	0.5401	0.4066	0.4374	0.6900	0.5309	0.5186
S.E.	0.3360	0.4081	0.2393	0.4627	0.2494	0.4181	0.2241	0.5558	0.2551	0.4558
Unloading										
Mean	0.3951	0.4418	0.5369	0.5369	0.5803	0.4623	0.4085	0.4651	0.4256	0.4723
S.E.	0.1462	0.1953	0.1953	0.1958	0.2732	0.2796	0.1527	0.1344	0.2657	0.4971
4%										
Loading										
Mean	0.4744	0.4311	0.5877	0.5748	0.6219	0.6085	0.5737	0.5308	0.7555	0.6248
S.E.	0.2418	0.1826	0.3183	0.2642	0.1457	0.2261	0.1555	0.2209	0.6799	0.2897
Unloading										
Mean	0.6349	0.4479	0.4942	0.4768	0.5001	0.5498	0.5707	0.7520	0.6217	0.5343
S.E.	0.4939	0.2236	0.3249	0.1760	0.3342	0.2003	0.2229	0.3198	0.3116	0.1739
6%										
Loading										
Mean	0.3310	0.3586	0.3077	0.4052	+	0.3732	0.3743	0.2547	0.3465	0.2963
S.E.	0.3214	0.2106	0.1660	0.2566	+	0.2202	0.1621	0.1507	0.1983	0.1721
Unloading										
Mean	0.3702	0.3608	0.3533	0.4253	+	0.3100	0.3521	0.3224	0.3501	0.2532
S.E.	0.2588	0.1517	0.1636	0.3085	+	0.1391	0.1797	0.1854	0.2198	0.1247

+For the 6% strain level tests, the fifth cycle occurs at 12s.

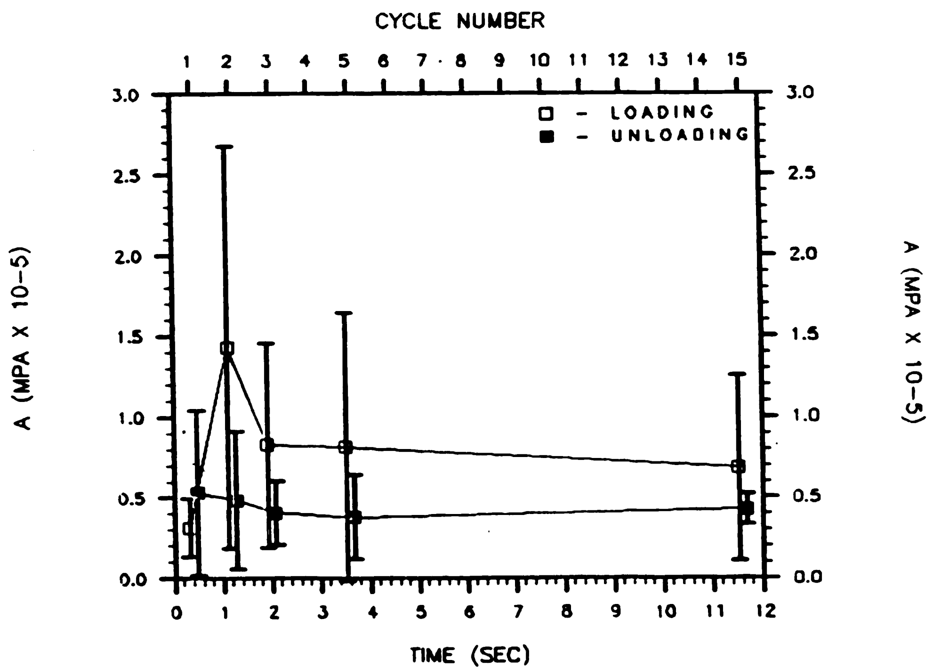

Figure 37 - The initial response of the power coefficient A for the 2% strain level.

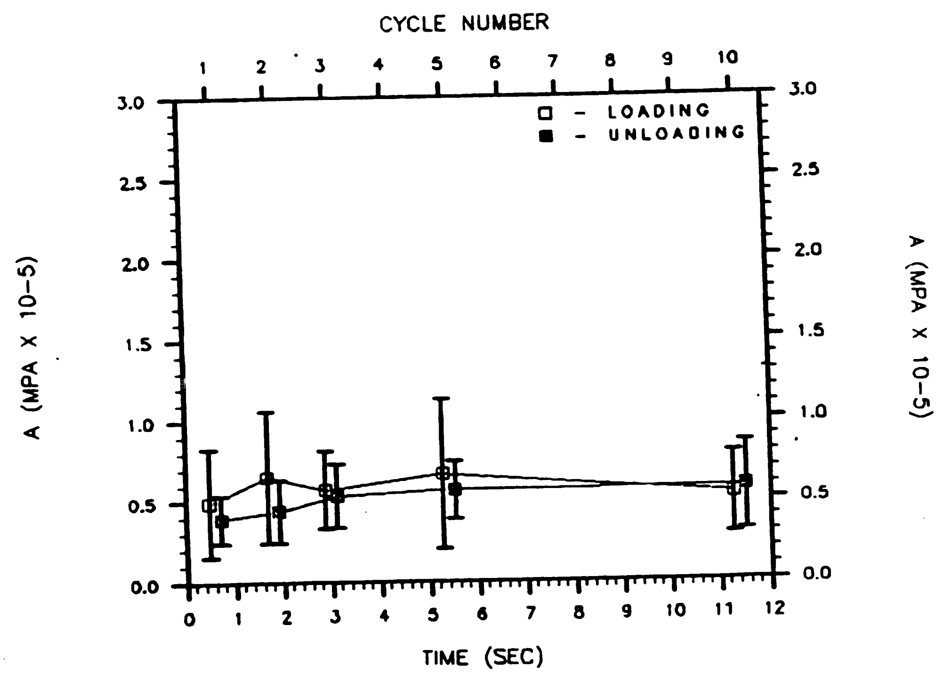

Figure 38 - The initial response of the power coefficient A for the 3% strain level.

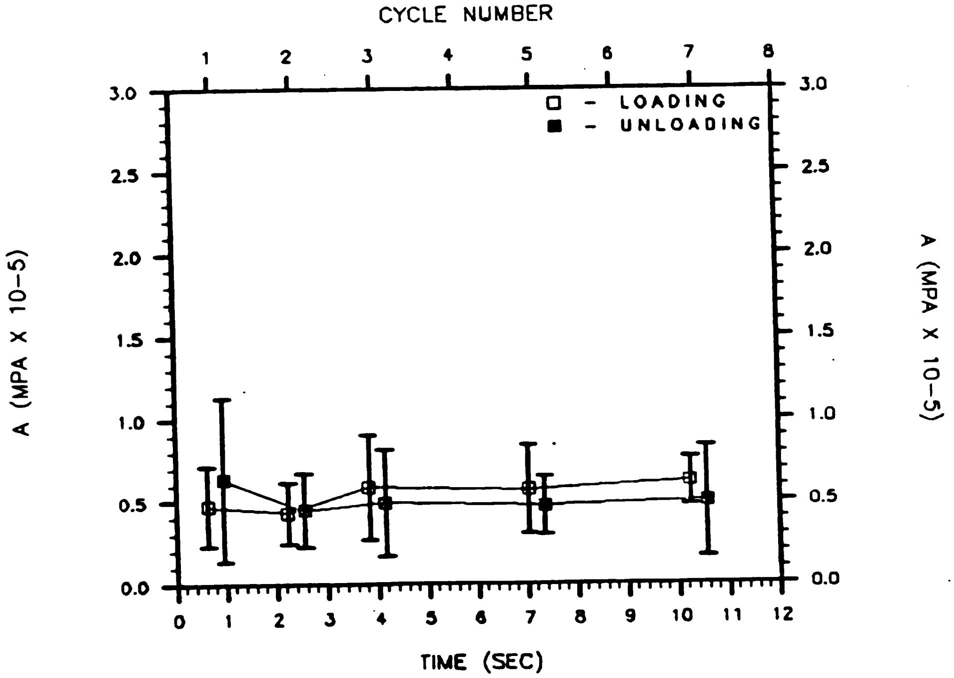

Figure 39 - The initial response of the power coefficient A for the 4% strain level.

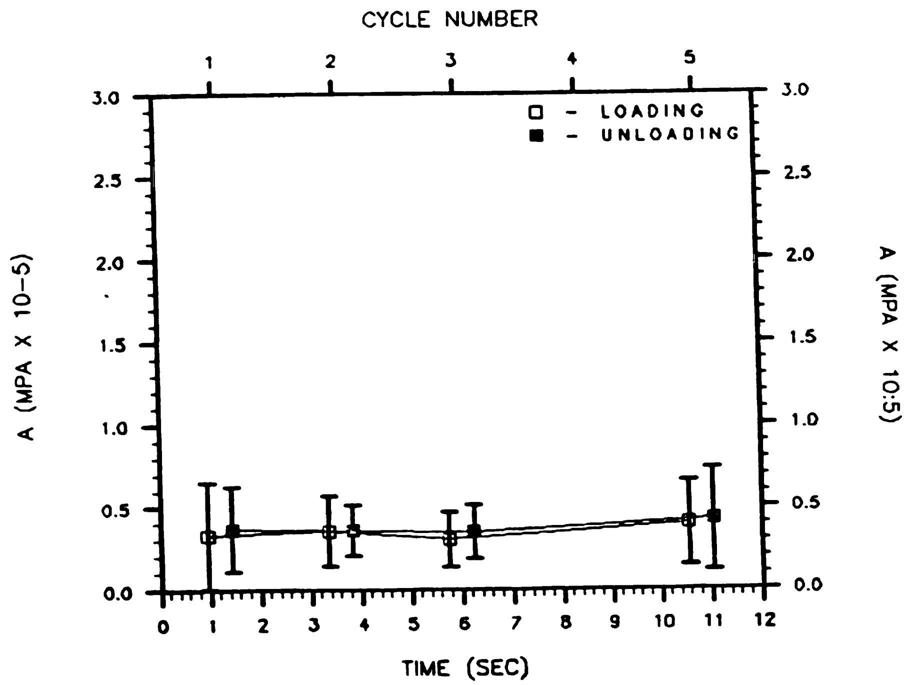

Figure 40 - The initial response of the power coefficient A for the 6% strain level.

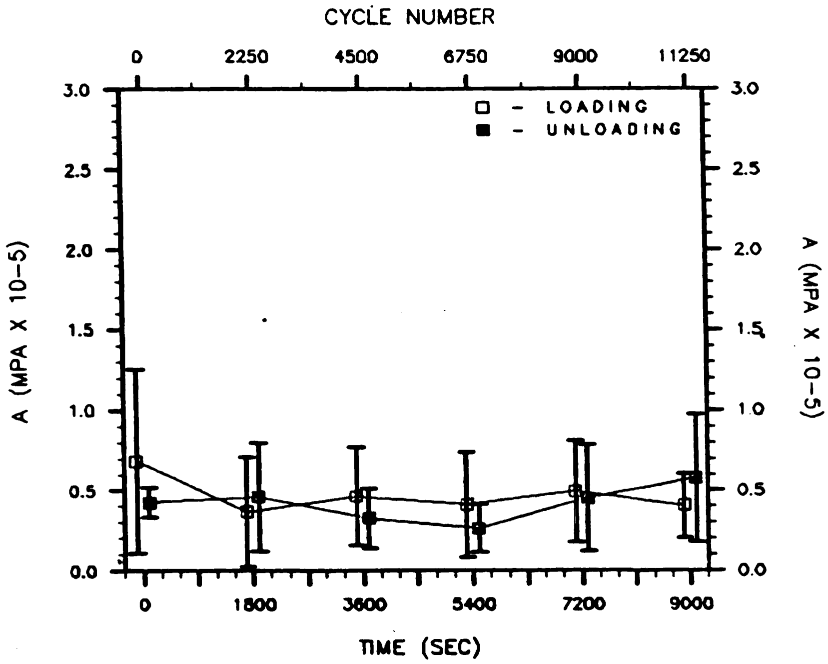

Figure 41 - The long term response of the power coefficient A for the 2% strain level.

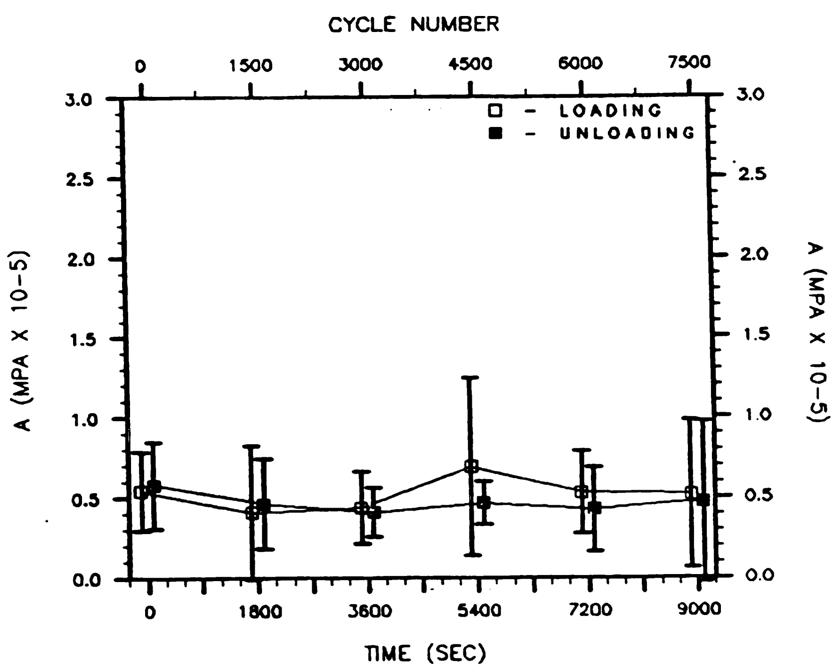

Figure 42 - The long term response of the power coefficient A for the 3% strain level.

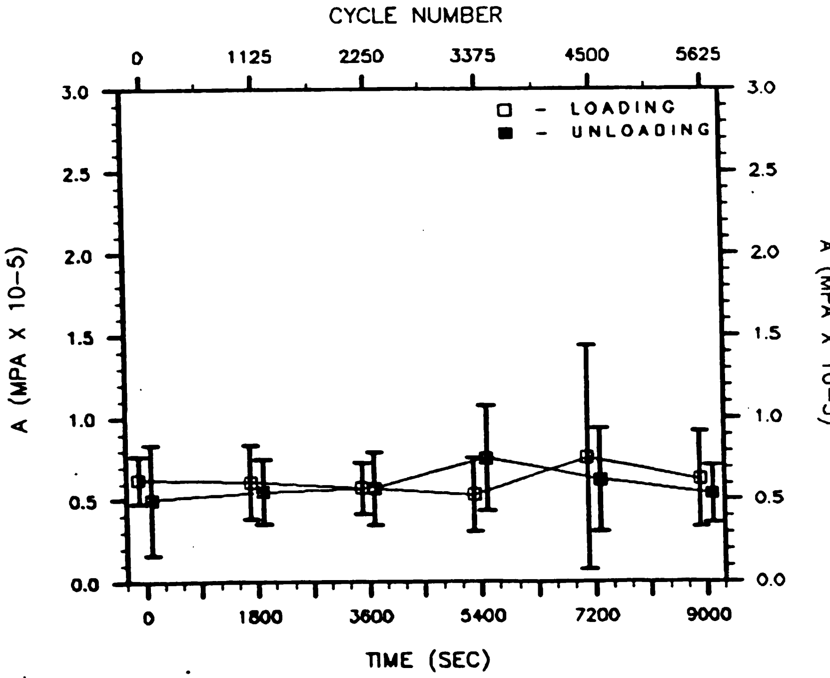

Figure 43 - The long term response of the power coefficient A for the 4% strain level.

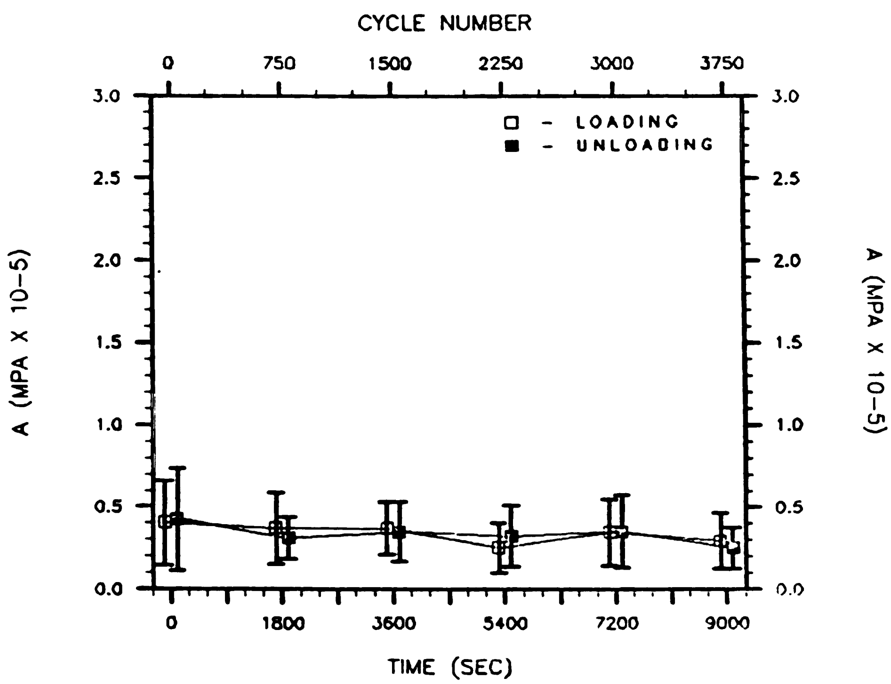

Figure 44 - The long term response of the power coefficient A for the 6% strain level.

TABLE 15 - Significant differences Between Strain Levels for A*

	Strain Level Interval Tested*					
	6%-4%	6%-3%	6%-2%	4%-3%	4%-2%	3%-2%
<u>Loading</u>						
1st Cycle	N	N	N	N	N	N
Last Cycle	N	N	N	N	N	N
1800s	N	N	N	N	N	N
3600s	N	N	N	N	N	N
9000s	N	N	N	N	N	N
<u>UnLoading</u>						
1st Cycle	N	N	N	N	N	N
Last Cycle	N	N	N	N	N	N
1800s	N	N	N	N	N	N
3600s	N	N	N	N	N	N
9000s	Y	N	N	N	N	N

*Behren-Fisher test (p=0.05) using Cochran and Cox estimates for the critical values [27].
**N indicates no significant difference, Y does.

TABLE 16 - Repeated Measures for A*

Loading	Cycles 1-2	Cycles 2-3	Cycles 3-5	Cycle 5 12s	12s -1800s	1800s -3600s	3600s -5400s	5400s -7200s	7200s -9000s	1800s -9000s	12s -9000s
2%	Y	N	N	N	N	N	N	N	N	N	Y
3%	N	N	N	N	N	N	N	N	N	N	Y
4%	N	N	N	N	N	N	N	N	N	N	Y
6%	N	N	N	+	N	N	N	N	N	N	Y
2%	N	N	N	N	N	N	N	N	N	N	Y
3%	N	N	N	N	N	N	N	N	N	N	Y
4%	N	N	N	N	N	N	N	N	N	N	Y
6%	N	N	N	+	N	N	N	N	N	N	Y

*Tau test, p=0.05
+For the 6% strain level tests, the fifth cycle occurs at 12s.

Table 17 lists the results for the power coefficient B for all strain levels. Figures 45-48 show the initial response for B at 2%, 3%, 4%, and 6% strain levels, respectively. Scatter in the B results is substantially smaller than for A. In general, the data behavior is similar to the slack strain data; with differences between the loading and unloading data diminishing with time. Greater increases occur in the loading curves. Figures 49-52 depict the long term B results for the 2%, 3%, 4%, and 6% strain levels, respectively. Here, as in the slack strain, a large increase in both the loading and unloading data occurs from 12s to 1800s. However, greater increases occur at lower strain levels here. The overall values for B increase with a decrease in strain level. This increase can be easily seen for the loading data in Figure 53, and for unloading data in Figure 54. Larger increases occur at both the 1st cycle-9000s and 1800-9000s intervals for the loading and unloading data data at lower strain levels.

In Table 18, the mean proportional ranges for all B data are listed. For the loading data, all mean proportional ranges increase with a decrease in strain level. The unloading data behaves similarly, with the exception from 1800s to 9000s, which behaves oppositely. This result indicates that greater changes in the unloading B occur past 1800s at higher strain levels. Overall, it appears that not only does the B decrease with an increase in strain level, but greater changes occur during testing at the lower strain levels.

Statistical results for B are listed in Table 19. Significant differences occur for the loading data at all strain level intervals for most cycles, with the exception of the 4%-3% and 6%-3% intervals.

TABLE 17 - Results for B (unitless)

	Cycle #1	Cycle #2	Cycle #3	Cycle #5	12s	1800s	3600s	5400s	7200s	9000s
2%										
Loading										
Mean	4.1320	4.0210	4.5140	4.6140	4.8290	6.1070	5.9470	6.1070	5.9875	6.2070
S.E.	0.5368	0.3728	0.4209	0.4191	0.6023	0.4224	0.6424	0.8727	0.9545	0.7626
Unloading										
Mean	5.3610	5.2280	5.4010	5.4710	5.5306	6.2870	6.5970	6.7570	6.4800	6.2850
S.E.	1.3120	0.5410	0.6848	0.4143	0.8209	0.4673	0.8779	1.6670	0.6362	0.5117
3%										
Loading										
Mean	3.1760	3.6350	3.7420	3.7970	3.9597	4.8090	4.7240	4.5740	4.6820	4.8180
S.E.	0.5795	0.7209	0.8040	0.8710	0.8889	1.1150	1.0860	0.8771	0.8645	1.1023
Unloading										
Mean	4.2650	4.2660	4.2150	4.1880	4.2930	5.0580	5.1906	5.1750	5.3810	5.1980
S.E.	0.7988	0.7444	0.8191	0.7809	0.7071	0.8692	0.9170	0.9125	0.9727	0.8834
4%										
Loading										
Mean	3.4803	4.0260	4.1757	4.2360	4.5970	4.8570	4.9510	5.0830	4.9510	5.0060
S.E.	0.4983	0.4613	0.4469	0.4412	0.7926	0.6788	0.5041	0.8048	0.8614	0.5482
Unloading										
Mean	4.3398	4.5950	4.6010	4.5992	4.6880	5.1220	5.1904	5.0740	5.2387	5.3410
S.E.	0.5136	0.6046	0.6869	0.5564	0.5690	0.5611	0.7308	0.6657	0.6635	0.6178
6%										
Loading										
Mean	2.9949	3.3715	3.5311	3.4414	+	3.8740	3.8596	4.1030	3.9880	3.9163
S.E.	0.1749	0.3630	0.3647	0.3111	+	0.5042	0.3274	0.4242	0.5984	0.6989
Unloading										
Mean	3.5280	3.6670	3.6097	3.5780	+	4.0870	4.0567	4.1536	4.1126	4.1400
S.E.	0.3481	0.3996	0.4760	0.3318	+	0.5221	0.2620	0.5234	0.4326	0.3691

+For the 6% strain level tests, the fifth cycle occurs at 12s.

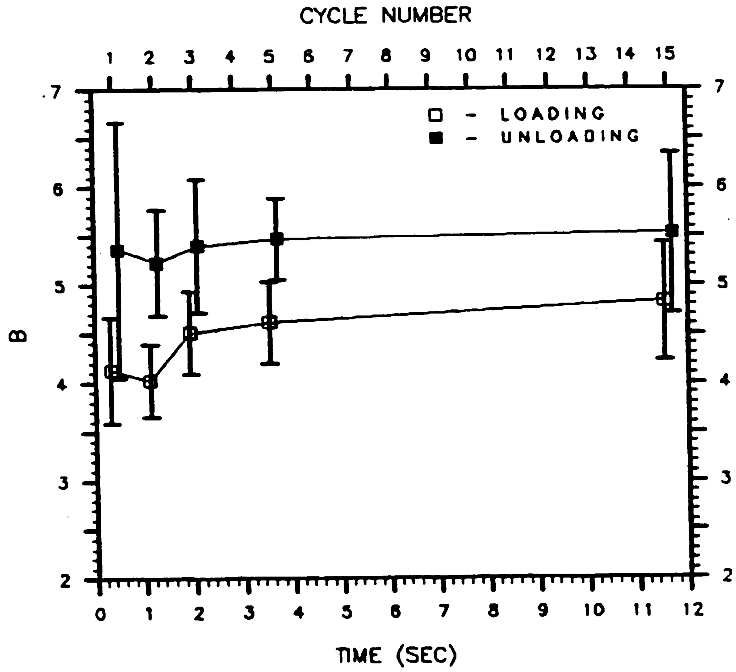

Figure 45 - The initial response of the power coefficient B for the 2% strain level.

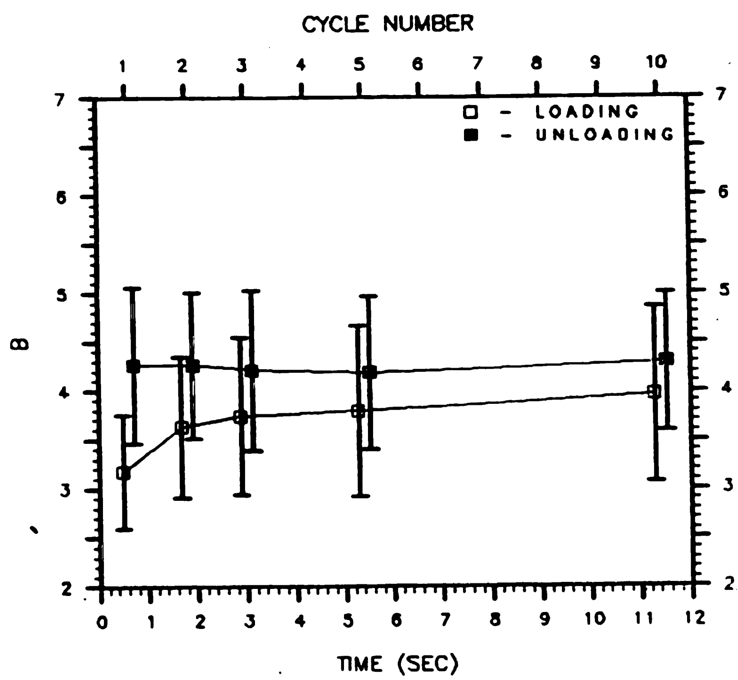

Figure 46 - The initial response of the power coefficient B for the 3% strain level.

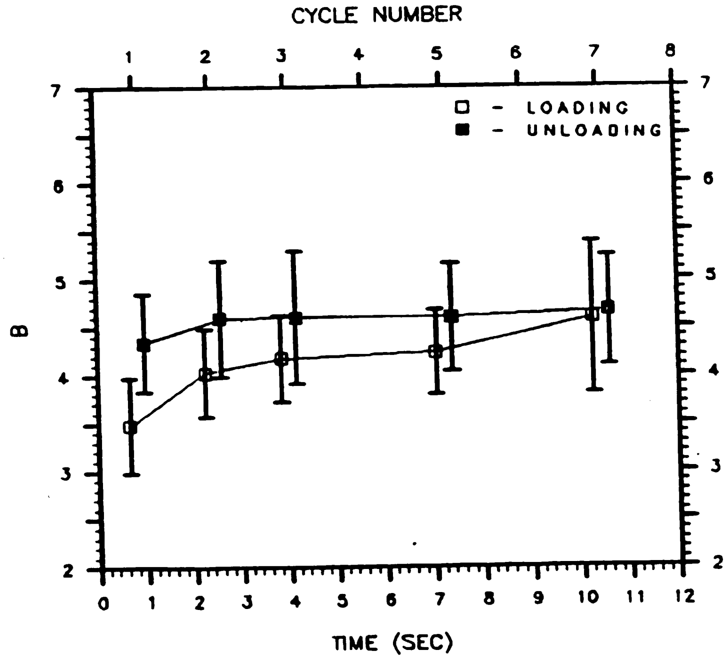

Figure 47 - The initial response of the power coefficient B for the 4% strain level.

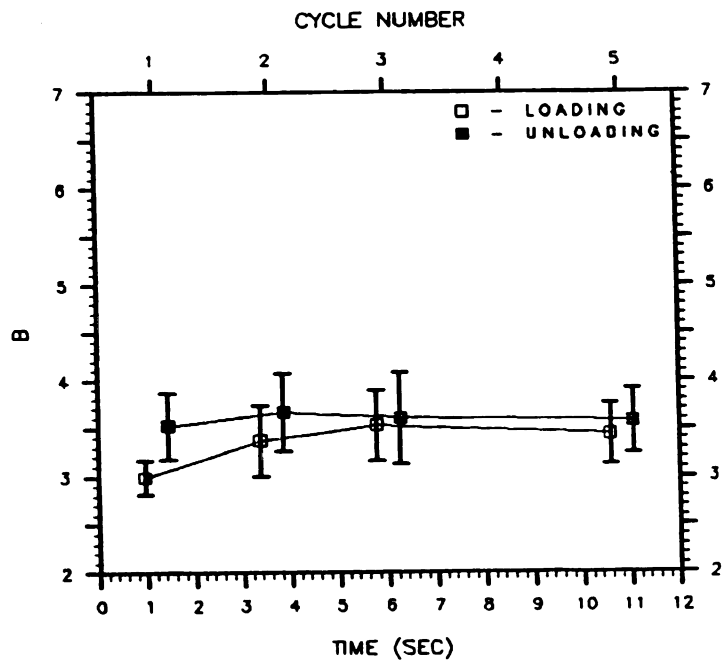

Figure 48 - The initial response of the power coefficient B for the 6% strain level.

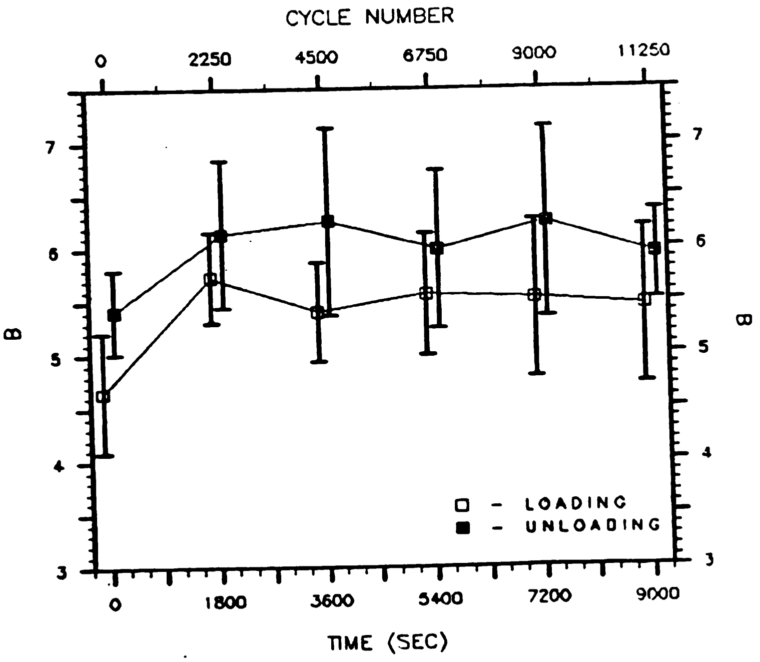

Figure 49 - The long term response of the power coefficient B for the 2% strain level.

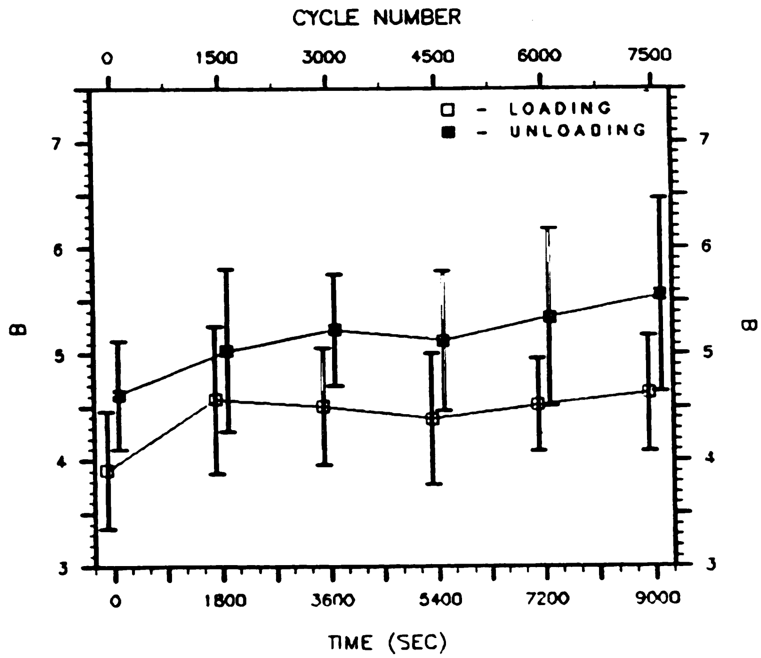

Figure 50 - The long term response of the power coefficient B for the 3% strain level.

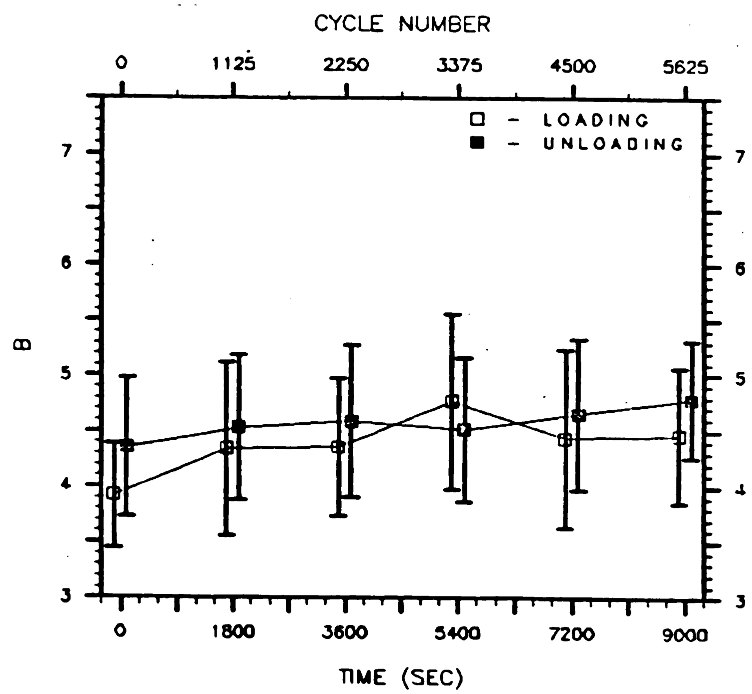

Figure 51 - The long term response of the power coefficient B for the 4% strain level.

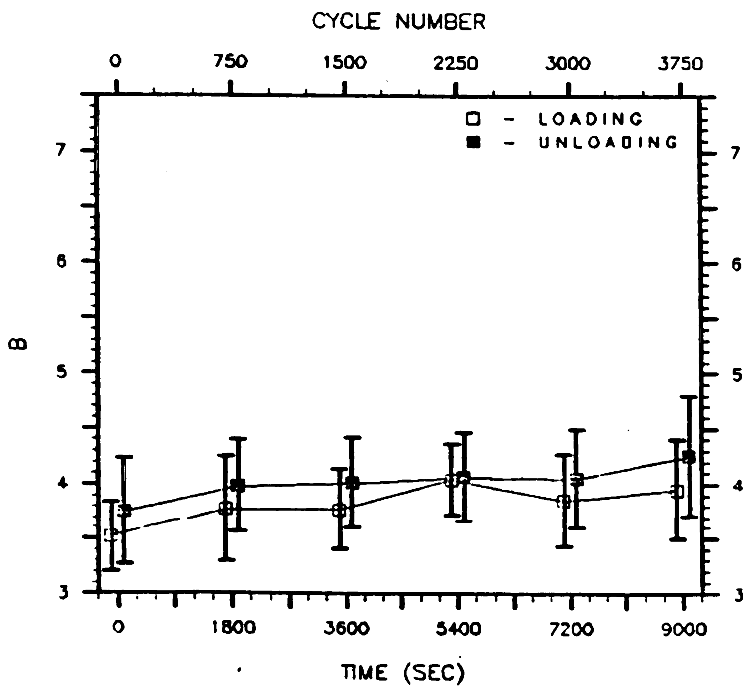

Figure 52 - The long term response of the power coefficient B for the 6% strain level.

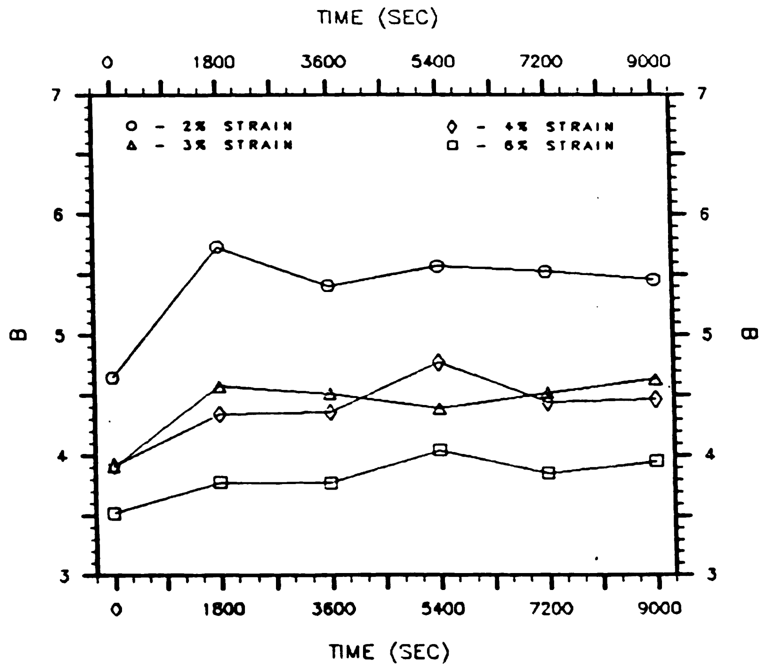

Figure 53 - The long term response of the loading power coefficient B for all strain levels.

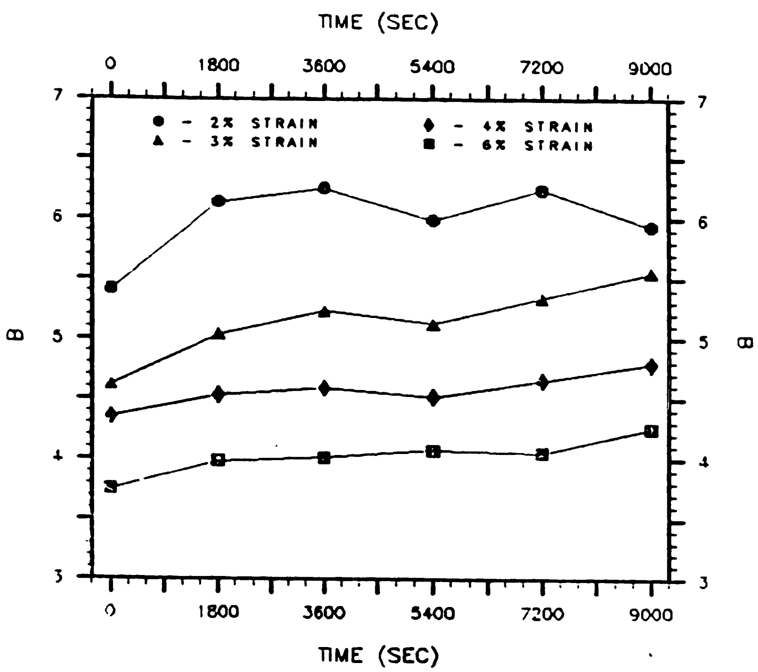

Figure 54 - The long term response of the unloading coefficient B for all strain levels.

TABLE 18 - Mean Proportional Changes in B (%)

Loading B

Strain Level	1st Cycle-9000s	1st Cycle-12s	12s-1800s	1800s-9000s
2%	1.0375	0.6390	0.6890	0.0500
3%	0.5473	0.2831	0.2861	0.0030
4%	0.3814	0.0650	0.1023	0.0373
6%	0.1536	0.0721	0.0792	0.0071

Unloading B

Strain Level	1st Cycle-9000s	1st Cycle-12s	12s-1800s	1800s-9000s
2%	0.4620	0.0848	0.3772	0.0010
3%	0.3110	0.0093	0.3017	0.0467
4%	0.2503	0.0871	0.1633	0.0548
6%	0.1020	0.0083	0.0937	0.088

TABLE 19 - Significant differences Between Strain Levels for B*

	Strain Level Interval Tested**					
	6%-4%	6%-3%	6%-2%	4%-3%	4%-2%	3%-2%
Loading						
1st Cycle	Y	N	Y	N	Y	Y
Last Cycle	Y	N	Y	N	N	Y
1800s	Y	Y	Y	N	Y	Y
3600s	Y	N	Y	N	Y	Y
9000s	Y	N	Y	N	Y	Y
UnLoading						
1st Cycle	Y	Y	Y	N	N	N
Last Cycle	Y	Y	Y	N	Y	Y
1800s	Y	Y	Y	N	Y	Y
3600s	Y	Y	Y	N	Y	Y
9000s	Y	Y	Y	N	Y	Y

*Behren-Fisher test ($p=0.05$) using Cochran and Cox estimates for the critical values [27].
**N indicates no significant difference, Y does.

The unloading data behaves similarly, except that the 6%-3% interval is significantly different. The lack of a significant difference at 4%-3% interval for all the B data could be due to either the values for B within this interval are nearly identical, or to excessive noise. The latter may be more probable since a significant difference also does not occur at the 6%-3% interval. Repeated measures for B, listed in Table 20, indicate significant differences occur only for the loading data between 1st and 2nd cycle, and for both loading and unloading data between 12s and 1800s. Although the 6% strain level tests show periodic significant differences past 1800s, no significant difference occurs from 1800 to 9000. Close inspection of the 6% strain level mean values, listed in Table 14, indicated a steady rise in B until 7200s, where B tends to drop slighly for both the loading and unloading data. This slight drop in B would explain why periodic significant differences occur at 6% strain past 1800s, but does not occur between 1800s and 9000s. This drop could be due to fiber or fibril damage, or grip slippage occuring past 5400s in the sample at 6% strain, but proof of this conjecture is beyond the scope of this study. The remaining strain levels show no significant differences past 1800s and between 1800s and 9000s, indicating no significant changes past 1800s. All strain levels show significant differences between 12s and 9000s, but none in the first data group past the first cycle. Evidently, changes in B are only large enough to show a significant difference between 12s amd 1800s and between the 1st and 2nd cycle for the loading B. These results imply the greatest increases in B are in the first half-hour, and that a rapid change occurs initially for the loading curve.

TABLE 20 - Repeated Measures for B*

	Cycles 1-2	Cycles 2-3	Cycles 3-5	Cycle 5 12s	12s -1800s	1800s -3600s	3600s -5400s	5400s -7200s	7200s -9000s	1800s -9000s	12s -9000s
<u>Loading</u>											
2%	N	Y	N	Y	Y	N	N	N	N	N	Y
3%	Y	N	N	N	Y	N	N	N	N	N	Y
4%	Y	N	N	N	Y	N	N	N	N	N	Y
6%	Y	N	N	+	Y	N	Y	N	Y	N	Y
<u>Unloading</u>											
2%	N	N	N	N	Y	N	N	N	N	N	Y
3%	N	N	N	N	Y	N	N	N	N	N	Y
4%	N	N	N	N	Y	N	N	N	N	N	Y
6%	N	N	N	+	Y	N	N	N	N	N	Y

*Tau test, p=0.05
+For the 6% strain level tests, the fifth cycle occurs at 12s.

The higher values for B at lower strain levels could be due to the nature of the stress-strain curve. A higher strain level test would include more of Region III, where the local value for B would be one. Hence, the overall value for B for the entire curve would be reduced with an increase in strain level. A further investigation of the stress-strain curve would be necessary to confirm this. The lower values reported by Haut and Little [5] are most probably due to offsets of 1 to the stress-strain data used in the power fit for this study. These offsets cause the least squares regression equation to yield a larger value for the power coefficient B, and a smaller A. It is possible that strain rate and strain level effects also influenced the power fit coefficients. Haut and Little [5] had a maximum strain of 1.8%, and a maximum strain rate of 0.68%/s, as opposed to 2% to 6% strain and a strain rate of 5%/s used here. Hubbard, et. al. [16] indicated some strain rate sensitivity for human tendon in the peak stress, loading M.T.M., and the hysteresis. However, no curve fitting was done, so a direct comparison is not possible. A future investigation of the strain rate sensitivity of tendon is necessary to explore the power fit coefficient results further.

Greater increases in B at lower strain levels could be explained by changes in the microstructure of the tendon. As stated in the introduction, changes in the microstructure of the tendon occur during the preconditioning cycles. Also, the stability of these changes past preconditioning has not been well documented. An increase in alignment could continue throughout the test, causing changes in the stress-strain curve primarily in Region II. This improved alignment would cause a larger value for B in Region II. Since the lower strain levels are mostly in this Region, they would experience larger changes in B. Also, the effect of this continually improving alignment would be less prominate at higher strain levels, since they contain proportionally less of Region II. Further support of this explanation is beyond this study, but continued changes in the stress-strain curves at all strain levels indicate some structural changes occur.

G. Histology

Histological results indicate continuous, unruptured fibers throughout the gripped and non-gripped sections. The griped sections were always very compressed, but neither broken nor torn, as discussed for the preliminary tests in the materials and methods section. The only problem area in the samples were in the grip-nongripped section interface. The fibers here appeared to be somewhat ruptured and flared, and not uniform. This could be due to the fact that the fibers rise out of the plane of the thinner gripped section to meet the thicker non-gripped section, hence appering to be broken. However, some damage to the tendon may have occured here. Further investigation of the condition of the fibers was not possible with the histological techniques used. In general, except for the compressed fibers in the gripped ends, no fiber damage could be seen in the histological slides.

H. Photographic Measurements

Photographic measurements, listed in Table 21, are shown as percent increases from the initial length right before testing and the final length right after testing. Large scatter is seen throughout the results, but there appers to be greater elongations of the specimens near the gripped ends. In one case, the ends of the tendon

TABLE 21 - Photograghic Results

Percent Increase in tendon length section from before just to after testing

Grip to Grip	Upper Grip to Dot	Lower Grip to Dot	Dot to Dot
2.22	2.82	*5.97	0.59
2.03	-	1.77	4.55
0.92	1.90	3.11	-0.41
2.28	2.35	*8.90	-0.08
10.55	*15.25	*7.55	0.97
0.59	0.74	1.25	0.65
1.17	*8.92	1.19	0.05
3.74	3.97	*8.78	3.61
1.07	*14.91	*10.99	-1.09
2.17	1.31	0.98	1.76
0.25	0.61	*3.42	0.02
0.81	*4.36	0.00	0.78
0.48	*5.08	-2.06	0.25
0.48	1.15	0.45	0.22
2.75	*10.36	*14.45	0.63

*Excessive Elongation

elongated 10% more than the middle section. Due to operational problems with the camera, the tests which corresponded to each photo was unknown, and several photo series were lost. However, the available results indicate that some slippage or damage in or near the grips may have occured. It is not possible to determine the exact influence these larger elongations near the grip ends had on the results. It is possible that some of the scatter seen in the data was caused by the mechanism which caused the greater elongation near the grips.

IV. CONCLUSION

Although the gripping method used in this study appeared to be adequate initially, photographic measurement results indicate possible damage to the tendon in or near the grips. The compression of the tendon within the grips may have caused some damage to the tendon, unobservable by the histological techniques used. Such damage could cause excessive elongation near the grips, since breakage would decrease the number of fibers bearing load, inducing greater stresses on these loaded fibers. Further development of gripping, elongation measurement and histological techniques are needed to better insure the validity of the results.

The most rapid changes in the mechanical response of the tendon took place in the initial part (first 12s) of the test. Substantial decreases the peak stress, unloading M.T.M., hysteresis; as well as increases in the loading MTM, slack strain, and the power fit coefficient B were greatest in this initial section. The changes in the above mechanical parameters indicate that the stress-strain curves have a marked tendency to "close-up" (i.e. difference between the loading and unloading curves diminish) in the initial section of the test. This is particularly evident in the decreasing differences in the loading and unloading M.T.M., B, slack strain, and the sharp initial decrease in the hystersis. This initial part corresponds to preconditioning, and the changes are virtually idential to the rapid changes discussed earlier for preconditioning. These large changes imply that some type of change in the tendon's structure must occur in the initial section of the test.

For the long-term response, the largest changes in the mechanical response occured between the initial 12s of the test and 1800s later. Continued increases in the power fit coefficient B and the slack strain occured, but to a less extent than in the initial part. The MTM, peak stress, and the hysteresis continued to decrease, also to a less extent.

Past 1800s, the changes diminished even further. The hysteresis essentially stabilized to about 16% for all strain levels past 1800s. Changes in the other mechanical parameters reduced throughout the rest of the test. The tendency for the stress-strain curves to "close-up" further appears not to occur significantly past 1800s, although continued changes in the power fit coefficient B indicates continued changes in the stress-strain curves in both the loading and unloading parts of the stress-strain curve.

Generally, results for the stabilization time indicate a strain level sensitivity; higher strain levels induce a longer stabilization time. It must be emphasized that the precise time for stabilization depends on the exact criteria used. Although the t-test criterion indicated no significant sensitivity to strain level for stabilization of the peak stress, it did show an overall rise in the stabilization for the M.T.M. data. The 2% and 5% difference criteria, usable only for a peak stress, also indicated an overall increase in stabilization time with an increase in strain level. Evidently, a higher strain level induces longer continued changes in the peak stress and the M.T.M.

For the other mechanical parameters, only the power fit coefficient B showed a strain level sensitivity. Total increases in the slack strain appear to be proportionally the same throughout the strain levels tested, and the hysteresis showed no detectable change at different strain levels. The B showed a significant rise in value with a decrease in strain level, as well as greater increases within a test at lower strain levels. The exact cause for this behavior is not known, but it is conjectured that it is due to a possible continued changes in the stress-strain curve in Region II during the test, which would effect the power fit coefficients more at lower strain levels.

In conclusion, changes in the mechanical response of the tendon continue throughout the test, and appear to take longer to stabilize with an increase in strain level. The most rapid changes occur at the beginning of the test, with continuing changes diminishing with time. Clearly, the preconditioning assumption does not precisely hold for long term cyclic extensions. Although the overall response appeared to visually stabilize initially, the long term B, M.T.M., slack strain, and peak stress indicate that this does not happen.

Recommendations for future studies include:

1. Improve the gripping technique to better insure that no damage is done to the samples.

2. A closer investigation of the initial 1800s of the test, especially for the hysteresis behavior.

3. Extend the strain level range to include lower strain levels (e.g. 0.5%, 1%).

4. Investigate cyclic creep at various stress levels, and compare to the results in this study.

5. Optically monitor sample extensions at different intervals along the samples.

It is hoped that this initial study will further the knowledge of the mechanical response of connective tissues.

APPENDICES

Appendix A

Ringers Lactate Solution

For a 20 liter container:

1. NaCl: 170.36 g.
2. KCl: 7.95 g.
3. CaCl (dehydrate): 4.73 g.
4. Sodium Lactate: 58.67 g.

Appendix B

Histology Method

Fixation

Tissue fixed three days in Mercuric chloride-formalin

Stock: NaCl 9 gm

$HgCl^2$ 70 gm

H_2O 1000 ml

Working:

9 parts stock: 1 part meutral formalin

On second day in fix tissue was trimmed and desired samples returned to fix.

Cleaning, infiltration and embedding

Tissues were processed through a graded series of alcohols to toluene followed by paraplast plus. This was done overnight on an autotechnican.

Tissues were embedding in paraplast plus (mp 56°C) embedding medium (Lancer).

Cutting:

Blocks were cut at 7μ on rotary microtome and sections mounted on slides. These were allowed to dry overnight at 37° before staining.

Staining:

Sections were stained with Hematoxylin-Eosin following standard H & E procedures. Harris Hematoxylin and Lipp's German Eosin were used although any standard H & E solutions will give good results.

BIBLIOGRAPHY

Bibliography

1. Fung, Y.C., "Stress-Strain History Relations of Soft Tissues in Simple Elongation," Biomechanics - Its Foundations and Objectives, eds. Fung, Perrone, and Anliker, Prentice Hall, New Jersey, 1972.

2. Viidik, A., "Mechanical Properties of Parallel Fibered Collageneous Tissues," Biology of Collogen, eds. Viidik, Vuust, Academic Press, London, 1980.

3. Viidik, A., "Interdependence between Structure and Function in Collagenous Tissues," Biology of Collogen, eds. Viidik, Vuust, Academic Press, London, 1980.

4. Crisp, J.D.C., "Properties of Tendon and Skin," Biomechanics - Its Foundations and Objectives, ed. Fung, Perrone, and Anliker, Prentice-Hall, New Jersey, 1972.

5. Haut, R.G., and Little, R.W., "A constitutive equation for collogen fibers," J. of Biomechanics, Vol. 5, 1972.

6. Butler, D.L. Grood, E.S., Noyes, F.R., "Biomechanics of Ligaments and Tendons," Exercise and Sports Science Review, ed. Hutton, R., Franklin Institute Press, Vol. 6, pp. 125-182, 1978.

7. Harkness, R.D., "Biological functions of collogen, " Biological Review, Vol. 36, 1981.

8. Yannas, I., "Collogen and geltin in the solid state," Rev. Macro mol. Chem., Vol. C7, p. 49, 1972.

9. Parington, F.R., and Wood, G.C., "The role of non-collogen components in mechanical behavior of tendon fibers," Biochem. Biophys. Acta, Vol. 69, pp. 485-495, 1963.

10. Haut, R.G., "Correlation Between Strain-Rate-Sensitivity in Rat Tail Tendon and Tissue Glycosaminoglycans," 1983 Biomechanics Symposium ASME 1983.

11. Elliot, P.M., "Structure and function of mammlian tendon," Biol. Rev., Vol. 40, pp. 342-421, 1965.

12. Diamant, J., Keller, A., Baer, E., Litt, M., and Arridge, R.G.C., "Collogen; ultrastructure and its relation to mechanical properties as a function of ageing," Proc. R. Soc. Lond., Vol. B180, pp. 293-315, 1972.

13. Viidik, A., "A rheological model for uncalcified parallel-fibered collageneous tissue," J. Biomech, Vol. 1, pp. 3-11, 1968.

14. Fung, Y.C., "Elasticity in Soft Tissue," Am. J. Physiol., Vol. 213, pp. 1532-1544, 1967.

15. Jenkins, R.B., Little, R.W., "A constitutive equation for parallel-fibered elastin tissue," J. Biomech, Vol. 7, pp. 397-402, 1974.

16. Hubbard, R.P., Soutas-Little, R.W., "Mechanical Properties of Human Tendon and Their Age Dependence," Final Report to the Nat. Inst. on Aging, grant no. 5 R01 AF 01471-02, 1982, and submitted to J. Biomech. Eng., 1983.

17. Little, R.W., Hubbard, R.P., Slonim, A., "Mechanical Properties of Spinal Ligaments of Primates: Final Report," AFAMRL-TR-83-005, Air Force Aerospace Medical Research Laboratory, Wright-Patterson Air Force Base, Ohio, 1983.

18. Cohen, R.E., Hooly, C.J., McCrum, N.G., "Viscoelastic creep of collageneous tissue," J. Biomech.,, Vol. 9, pp. 175-183, 1976.

19. Woo., F. L-Y., Gomez, M.A., Akeson, W.M., "The time and history-dependent viscoelastic properties of the canine medial collateral ligament," J. Biomech. Eng., Vol. 103, pp. 293-298, 1981.

20. Little, R.W., Hubbard, R.P., Hyler, D.L., Slonim, A., "Mechanical Properties of Spinal Ligaments for Rhesus Monkey, Baboon, and Chimpanzee," AFA MRL-TR-81-40, Air Force Aerospace Medial Research Laboratory, Wright-Patterson Air Force Base, Ohio, 1981.

21. Guth, E., Wack, P.E., and Anthony, R.L., "Significance of the equation of state for rubber," J. Appl. Physics, Vol. 17, pp. 347-351, 1940.

22. Lanir, Y., "Structure-strength relations in mammilian tendon," J. Biophysics, Vol. 24, pp. 541-554, 1974.

23. Rigby, B.J., "Effect of cyclic extension on the physical properties of tendon collogen and its possible relation to biological ageing of collogen." Nature, Vol. 202, pp. 1072-1074, 1964.

24. "Mulplt", a graphics computer routine written by: Dr. T.V. Atkinson, Dept. of Chemistry, Michigan State University, East Lansing, MI, 48824.

25. Crow, E.I., Davis, F.A., Maxfield, M.A., "Statistics Manual," Dover, 1960.

26. Morrison, D.F., "Multi-Variate Statistical Methods," McGraw-Hill, 1976.

27. Winer, B.J., "Statistical Principles in Experimental Design", McGraw-Hill, 1962.

28. Selke, D.J., Little, R.W., Hubbard, R.P., "Mechanical Properties of Lower Limb Tendons and Ligaments in Primates," AFA MRL-TR-82-56, Air Force Aerospace Medial Research Laboratory, Wright-Patterson Air Force Base, Ohio, 1982.